



Far future climate (2060–2100) of the northern Adriatic air–sea heat transfers associated with extreme bora events

Cléa Denamiel¹ · Iva Tojčić¹ · Ivica Vilibić¹

Received: 22 May 2020 / Accepted: 18 August 2020 / Published online: 29 August 2020
© Springer-Verlag GmbH Germany, part of Springer Nature 2020

Abstract

The northernmost part of the Mediterranean Sea, the northern Adriatic shelf, is a complex area where the intensity of dense water formation and the consequent Adriatic-Ionian thermohaline circulation are shaped by a combination of extreme wintertime bora winds and substantial freshwater loads. To better understand the impact of global warming on extreme bora dynamics and the associated sea surface cooling, this study applies the Adriatic Sea and Coast (AdriSC) kilometer-scale modelling suite to the far future climate (2060–2100) period. Under both Representative Concentration Pathway (RCP) 4.5 and RCP 8.5 greenhouse emission scenarios, the AdriSC simulations are carried out via the combination of a statistical approach—consisting of an ensemble of 3-day simulations for 22 extreme bora events, and a pseudo-global warming (PGW) methodology—imposing a climatological change to the forcing used to produce the evaluation (present climate) runs. Despite a noteworthy decrease in intensity of the bora winds (by up to 3 m/s), the latent heat losses are simulated to increase (by up to 150 W/m²) due to the reduction in relative humidity in the northern Adriatic (by up to 3%). Consequently, the sea surface cooling associated with severe bora events and preconditioning the dense shelf water formation in the northern Adriatic is projected to not significantly change compared to present climate. Although these results need to be further confirmed, this study thus provides a new view on the future of processes driven by sea surface cooling, such as the dense shelf water formation or the Adriatic-Ionian thermohaline circulation, that were projected to decrease in the future climate by regional climate models an order of magnitude coarser than the AdriSC simulations.

Keywords Adriatic sea · Extreme bora wind events · Sea surface cooling · Pseudo-global warming · Far future climate

1 Introduction

Climate change, one of the most complex issues facing modern societies, will be felt worldwide for the decades and centuries to come, but even more along the coastal areas where it strongly impacts lagoons, fishing activities, aquaculture, tourism, etc. and could yield to a reduction of local food supply and economic security (Ionescu et al. 2009). In the Mediterranean Sea, a well-known hot-spot region for climate change (Giorgi, 2006), the impact of global warming has been principally studied with coupled atmosphere–ocean climate models at the global and regional scales. Notably, concerning the most recent publications, González-Alemán et al. (2019) simulated an increase in frequency of the

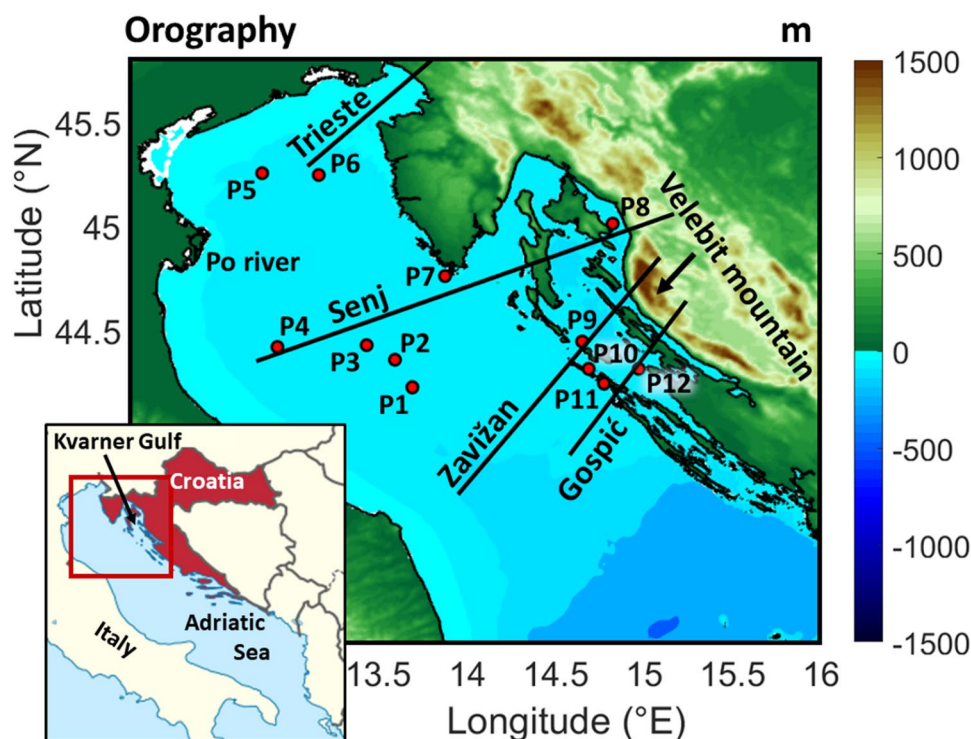
Mediterranean hurricanes (medicanes) under Representative Concentration Pathway (RCP) 4.5 scenario (van Vuuren et al. 2011) with resolutions of 25-km in the atmosphere and 100-km in the ocean, while Darmaraki et al. (2019) and Soto-Navarro et al. (2020) analyzed the projections under RCP 8.5, RCP 4.5 and RCP 2.6 scenarios of the Med-CORDEX ensemble using regional climate models with resolutions of at least 12-km in the atmosphere and 10-km in the ocean. They respectively found that, along the twenty-first century and independently of the choice of the emission scenario, marine heatwaves will be more frequent and water masses will become saltier, warmer and less dense.

However, in the northern Adriatic region (Fig. 1), the severe bora events—winds strongly influenced by the complex orography of the Velebit and other mountain ranges (Fig. 1), associated with hurricane-strength gusts up to 50 m/s (Belušić and Klaić 2004; Grisogono and Belušić 2009) and frequently occurring during the fall and winter seasons—can only be represented by kilometer-scale

✉ Cléa Denamiel
cdenamie@izor.hr

¹ Institute of Oceanography and Fisheries, Šetalište I.
Meštrovića 63, 21000 Split, Croatia

Fig. 1 Orography and bathymetry of the area of interest (red frame of the bottom left panel) along the northern Adriatic Croatian coastline with the location of the four cross-shore transects (Trieste, Senj, Zavižan and Gospić) and the 12 points (P1–P12) used to analyze the results



“limited area” meteorological models (Grisogono and Belušić 2009; Trošić and Trošić 2010; Prtenjak et al. 2010; Kuzmić et al. 2015; Josipović et al. 2018; Denamiel et al. 2020). Typical duration of bora events is about two days, but may reach a week, while having substantial variability at daily, hourly and sub-hourly timescales (Belušić et al. 2004; Grisogono and Belušić 2009; Stiperski et al. 2012). Additionally, the sea surface cooling, the mixing of the water column, the dense water formation and the thermohaline circulation driven by these extreme bora storms (Hopkins et al. 1999; Poulain and Raicich 2001; Artegiani et al. 1997; Orlić et al. 2007) can only be captured by coastal ocean models at a kilometer scale (Beg-Paklar et al. 2001; Pullen et al. 2006, 2007; Sherwood et al. 2004; Bignami et al. 2007; Boldrin et al. 2009; Carniel et al. 2009; Janeković et al. 2014; Ličer et al. 2016). As for the bora, the cooling occurs at hourly to daily timescale, rapidly impacting the vertical ocean structure in shallow areas already homogenized during the late autumn and winter seasons (Franco and Michelato 1992; Artegiani et al. 1997) and taking out heat from the sea at rates up to 2000 W/m^2 for the most extreme events (Janeković et al. 2014). In the following days to weeks, a strong thermohaline circulation develops in the Adriatic-Ionian basin and can last for months (Orlić et al. 2007). Therefore, sea surface cooling during wintertime bora may be considered as a proxy for the dense water formation and the associated thermohaline circulation, which have, for example, a critical impact on the ocean biogeochemistry (e.g. Conan et al. 2018).

So far, the future climate of the bora winds has been documented through an assessment of EURO-CORDEX climate models of 0.11° horizontal resolution (i.e. at a resolution an order of magnitude coarser than recommended) by Belušić Vozila et al. (2019). This study underpins a decrease of both intensity and frequency of the bora wind in the future climate, except in the northern Adriatic, however the wind regimes over such a complex mountainous region were found to be sensitive to orography and boundary conditions coming from global models. Regarding the Adriatic-Ionian thermohaline circulation, it has been documented to weaken in the present (Vilibić et al. 2013) and future (Somot et al. 2006) climates, although the latter should be taken cautiously as regional ocean climate models underestimate the dense water formation (Dunić et al. 2019). Thus, understanding the impact of climate change on the severe bora dynamics and the associated northern Adriatic air–sea exchanges requires the implementation and use of kilometer-scale coupled atmosphere–ocean climate models.

Following these demands, the modular approach implemented in the Adriatic Sea and Coast (AdriSC) modelling suite (Denamiel et al. 2019) has been designed to allow a great flexibility in investigating processes with various spatial and temporal scales in the Adriatic region. In particular, an ensemble of simulations has been recently created with the AdriSC model in order to study historical and climate projections of extreme storms (Denamiel et al. 2020) with resolutions varying from 15 to 1.5 km in the atmosphere and from 3 km to 10 m in the ocean. In the Adriatic Sea, where

most of the coupled atmosphere–ocean bora studies concentrated principally in reproducing single historical events (e.g. Pullen et al. 2006, 2007; Janeković et al. 2014; Ličer et al. 2016), this ensemble approach allowed for process-oriented statistics and has already provided meaningful insights concerning the known bora dynamics and the past and future of extreme wave climates (Denamiel et al. 2020).

The goal of this work is thus to study the impact of global warming, for the far future 2060–2100 period, on both the bora strength and dynamics and the associated air–sea surface heat transfer—strongly preconditioning the formation of dense shelf waters in the northern Adriatic Sea, using the representative ensemble of 22 extreme bora events reproduced by the AdriSC climate model simulations (with resolutions of 3-km in the atmosphere and 1-km in the ocean). For the future climate, the simulations were carried out imposing pseudo-global warming methodology (PGW; Schär et al. 1996; Denamiel et al. 2020). To this purpose, general information about the AdriSC modelling suite, set-up of the simulations for the present (hereafter referred as evaluation mode) and future (hereafter referred as climate projection mode) climates and the selected events used to create the ensemble and evaluate the models is first presented in Sect. 2. In Sect. 3, the main results of the study—projection of the bora conditions and the associated sea surface cooling under global warming derived from the AdriSC climate results—are analyzed for the ensemble of bora storms. Finally, some discussions and conclusions are drawn in Sect. 4.

2 Model and methods

The Adriatic Sea and Coast (AdriSC) kilometer-scale climate model (Denamiel et al. 2019, 2020) has been recently developed to accurately reproduce the atmospheric and oceanic climate processes over the Adriatic and northern Ionian Sea. The modelling suite relies on the use and development of the Coupled Ocean–Atmosphere–Wave–Sediment Transport (COAWST) modelling system (Warner et al. 2010)

built around the Model Coupling Toolkit (MCT) which exchanges data fields and dynamically couples the Weather Research and Forecasting (WRF) atmospheric model with the Regional Ocean Modeling System (ROMS). It is set-up with (1) two different nested grids of 15-km and 3-km resolution used in the WRF model and covering respectively the central Mediterranean area and the Adriatic-Ionian region and (2) two different nested grids of 3-km and 1-km resolution used for the ROMS model and covering respectively the Adriatic-Ionian region (similarly to the WRF 3-km grid) and the Adriatic Sea only. More details on the set-up of the AdriSC modelling suite—which is installed and fully tested on the European Centre for Middle-range Weather Forecast (ECMWF) high-performance computing facilities—can be found in Denamiel et al. (2019).

In this study, the impacts of climate change—under Representative Concentration Pathway (RCP) 4.5 and RCP 8.5 greenhouse gas projections—on the dynamics of the strongest bora storms recorded in the last 30 years, as well as on the associated sea surface cooling in the northern Adriatic Sea, are derived with the AdriSC modelling suite. As no public catalogue compiling the most severe bora storms exists in Croatia, the selection of the 22 events (spanning between 1991 and 2019) used hereafter has been derived from an in-depth bibliographical research including meteorological bulletins (in Croatian), local newspapers, photographs and videos, and listed by Denamiel et al. (2020).

In order to simulate, as efficiently as possible, these 22 selected historical storms and their climate projections—under both RCP 4.5 and RCP 8.5 scenarios—the AdriSC model has been set-up to run for short periods of three days with the last 24-h atmospheric and oceanic hourly results, including the peak of the storm. The atmospheric and oceanic variables were extracted from the WRF 3-km and ROMS 1-km models, respectively. As summarized in Table 1, in evaluation mode initial conditions and boundary forcing were provided by the 6-hourly ERA-Interim re-analysis fields (Dee et al. 2011; Balsamo et al. 2015) in the atmosphere and by the daily re-analysis MEDSEA-Ocean fields (Pinardi et al. 2003) in the ocean, while in climate

Table 1 Summary of the AdriSC climate component main features

	Atmosphere	Ocean
Models	WRF	ROMS
Number of domains	2	2
Resolution	15 km	3 km 3 km 1 km
Initial and boundary conditions	ERA-Interim (evaluation mode only) + LMDZ4 climatological changes (climate projection mode)	MEDSEA (evaluation mode only) + NEMOMED8 climatological changes (climate projection mode)
Duration of run (with d0 the day of the event at 0 h)	72 h from d0 – 48 h to d0 + 24 h	
Frequency of outputs	Hourly	

projection mode—i.e. RCP 4.5 and RCP 8.5 scenarios—the pseudo-global warming (PGW) methodology was implemented. The principle of the PGW simulations—as first introduced by Schär et al. (1996) for the atmosphere and extended to coupled atmosphere–ocean models by Denamiel et al. (2020)—is to impose an additional climatological change (e.g. a temperature change representative of the increase in temperature between past and future climate) to the forcing used to produce the evaluation runs. As presented by Denamiel et al. (2020), the atmospheric and oceanic climatological changes (between the 1979–2019 and the 2060–2100 periods) used to force the AdriSC RCP 4.5 and RCP 8.5 climate simulations presented in this study, have been extracted from the coupled atmosphere–ocean regional climate model LMDZ4-NEMOMED8 (Hourdin et al. 2006; Beuvier et al. 2010). Finally, even though the 48-h spin up may seem relatively short for a coupled atmosphere–ocean model, it has been previously demonstrated that the future of atmospherically-driven extreme events can be well represented within the PGW framework with spin up lower than 2 days (e.g. Trapp and Hoogewind 2016; Chen et al. 2020). The chosen spin up of the presented simulations is thus judged appropriate to properly represent the atmospheric dynamics and the resulting rapid sea surface cooling during extreme bora events in the northern Adriatic.

In terms of the AdriSC model skill to reproduce severe bora conditions, evaluations against in situ data have been successfully performed for the 10 m wind speed and direction, the 2 m temperature and dew point and the mean sea level pressure, as well as for the sea wave conditions (significant wave height, peak wave period and mean wave direction) in Denamiel et al. (2020). This study reveals that the AdriSC model is capable to reproduce the strongest bora dynamics, even though the WRF-3 km results tend to slightly overestimate (by about 10%) wind speeds below 15 m/s.

Finally, as quantifying the climate change impact on extreme bora strength and dynamics is one of the aims of this study, the strategy adopted to analyze the atmospheric results is:

- To identify and extract the peak of each storm for each mode—i.e. evaluation as well as RCP 4.5 and RCP 8.5 scenarios,
- To derive meaningful physical variables such as horizontal wind speed, vertical wind velocity, virtual potential temperature, potential vorticity (PV) and Froude number (Fr) at the peak of each storm and for each mode (see Appendix for more details),
- To define the extreme baseline RCP 4.5 and RCP 8.5 conditions, for each of these physical variables, as the median derived from the ensemble of the 22 WRF 3-km results,

- And to evaluate the climate impact on each of these physical variables—called climate adjustment hereafter, as the medians derived from the ensemble of the 22 differences between the peak conditions of RCP 4.5 and RCP 8.5 simulations separately and evaluation results.

Given the overall three-dimensional nature of the bora dynamics, these results are presented as horizontal slices from the surface conditions (at 5 m height following the terrain) to 2 km height every 0.5 km and vertical cross-sections (Fig. 1) extracted for four transects (starting near Trieste, Senj, Zavižan and Gospić), chosen where the bora jets were the strongest and the further extended offshore in the evaluation simulations. Additionally, in order to capture the impact of climate change on the sea surface cooling, the spatial variations of the RCP 4.5 and RCP 8.5 baseline and climate adjustment conditions of the minimum surface heat fluxes (decomposed as total, sensible and latent fluxes; see Appendix for more details) and the minimum sea surface temperature (SST) anomaly (defined as the difference between the hourly SST and the initial SST taken 24-h before each event) are derived from respectively the WRF 3-km and ROMS 1-km results. The distributions of the hourly surface heat fluxes and SST anomalies in evaluation and scenario (RCP 4.5 and RCP 8.5) modes are also analyzed for the ensemble of 22 events at 12 different locations (Fig. 1, points P1–P12) where the sea surface cooling was the most intense in evaluation mode.

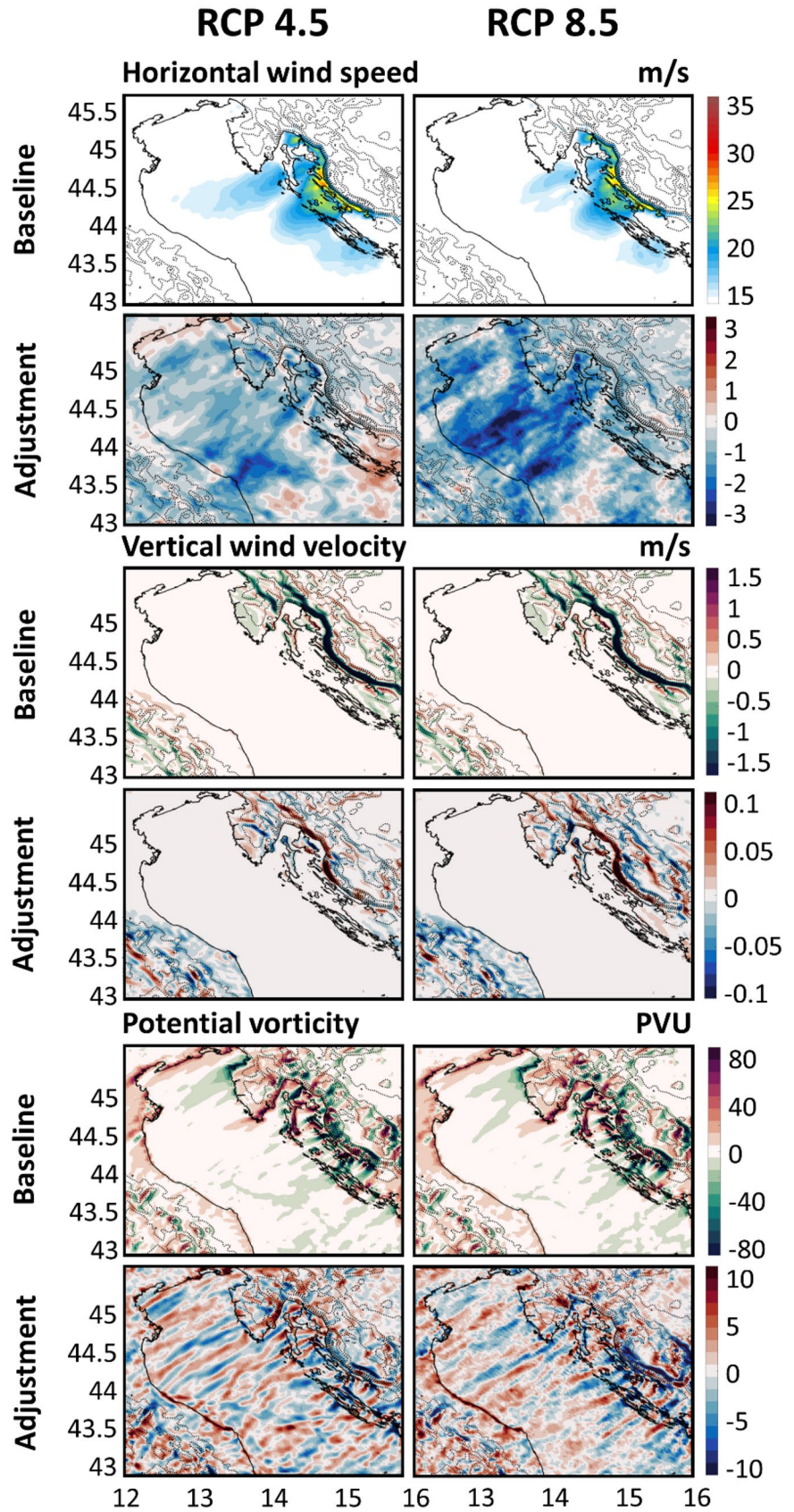
3 Results

3.1 Impact of climate change on extreme bora dynamics

To better understand the impact of climate change on the extreme bora simulations in the northern Adriatic for the 2060–2100 period, the WRF 3-km model RCP 4.5 and RCP8.5 baseline conditions (i.e. median of peak conditions) and climate adjustments (i.e. median of the difference between RCP 4.5 and RCP 8.5 separately and evaluation peak conditions) are presented as horizontal slices between the surface and 2 km of height (Figs. 2 and 3) and as vertical profiles for the four cross-shore transects (Figs. 4, 5, 6, 7 and 8).

Horizontally, the major known bora features can clearly be seen in the RCP 4.5 and RCP 8.5 baseline conditions derived from the WRF 3-km simulations. The wake and jet dynamics along the coast (Jiang and Doyle 2005; Belušić and Klaić 2006; Gohm et al. 2008; Signell et al. 2010) still exists in the climate projections with variations of the horizontal wind speed magnitude from north to south—i.e. intense jets above 20 m/s between the surface and 1 km

Fig. 2 Baseline RCP 4.5 and RCP 8.5 conditions (median of the scenario results) and climate adjustment (median of difference between scenario and evaluation results) for horizontal wind speed, vertical wind velocity and potential vorticity at the surface (about 5 m height) during the peak of 22 selected extreme bora events. Topographic contours are displayed every 250 m with dashed lines



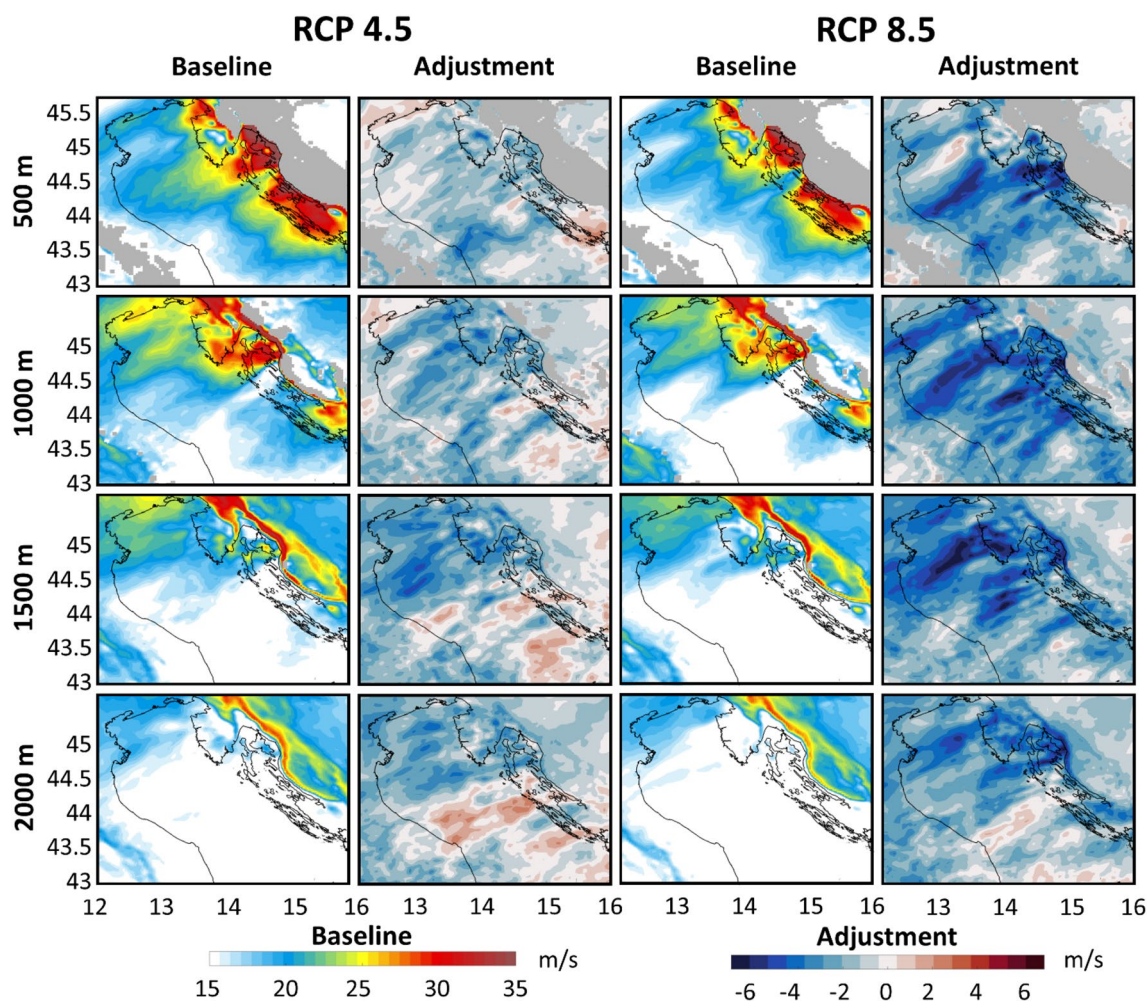


Fig. 3 Baseline RCP 4.5 and RCP 8.5 conditions (median of the scenario results) and climate adjustment (median of difference between scenario and evaluation results) for horizontal wind speed at heights

of 500 m, 1000 m, 1500 m and 2000 m during the peak of 22 selected extreme bora events

height separated by lower speeds (Figs. 2 and 3). However, the intensity of these bora jets largely decreases between the surface and 2 km height (Figs. 2 and 3), with climate adjustments up to -3.5 m/s and -6 m/s for RCP 4.5 and RCP 8.5 scenarios, respectively. As this decrease in intensity is not homogeneous, the location of the wakes and jets may also slightly vary between the future scenario (RCP 4.5 and RCP 8.5) and the evaluation conditions. To be noted, the Trieste jet—known to be overall less intense than the other jets along the Velebit mountain range, is projected to decrease down to 15 m/s near the surface in the climate projections and is thus not represented in Fig. 2.

The surface potential vorticity (PV) banners (i.e. the strip-shaped features of the PV field) associated with the alternation of the major mountain gaps and peaks—as described by Grubišić (2004)—are also maintained for both RCP 4.5 and RCP 8.5 climate projections (Fig. 2). The altering positive (up to 80 PVU = 10^{-6} m² K/s/kg) and negative (below

-80 PVU) potential vorticity banners are reproduced in the baseline simulation perpendicularly to the Velebit mountain range and associated with the main jet (negative) and wake (positive) structures along the coast. To be noted, as the PV is extracted at 5 m above the ground where friction is important, these values are overall larger than the ones presented in Grubišić (2004). Nonetheless, as for the wind speed, the intensity of the PV banners is modified under both RCP 4.5 and RCP 8.5 scenarios with climate adjustments of up to ± 10 PVU, denoting a weakening of alongshore PV gradients, particularly over the sea. Finally, the primary generation mechanism of extreme bora events—i.e. the atmospheric wave breaking (e.g. Klemp and Durran 1987; Grubišić 2004; Jiang and Doyle 2005; Gohm et al. 2008)—can also clearly be seen in the RCP 4.5 and RCP 8.5 baseline conditions (Fig. 2), with vertical velocities strongly negative along the lee of the Velebit mountain range (up to -1.5 m/s at surface) and positive along the coastline (about 0.5 m/s

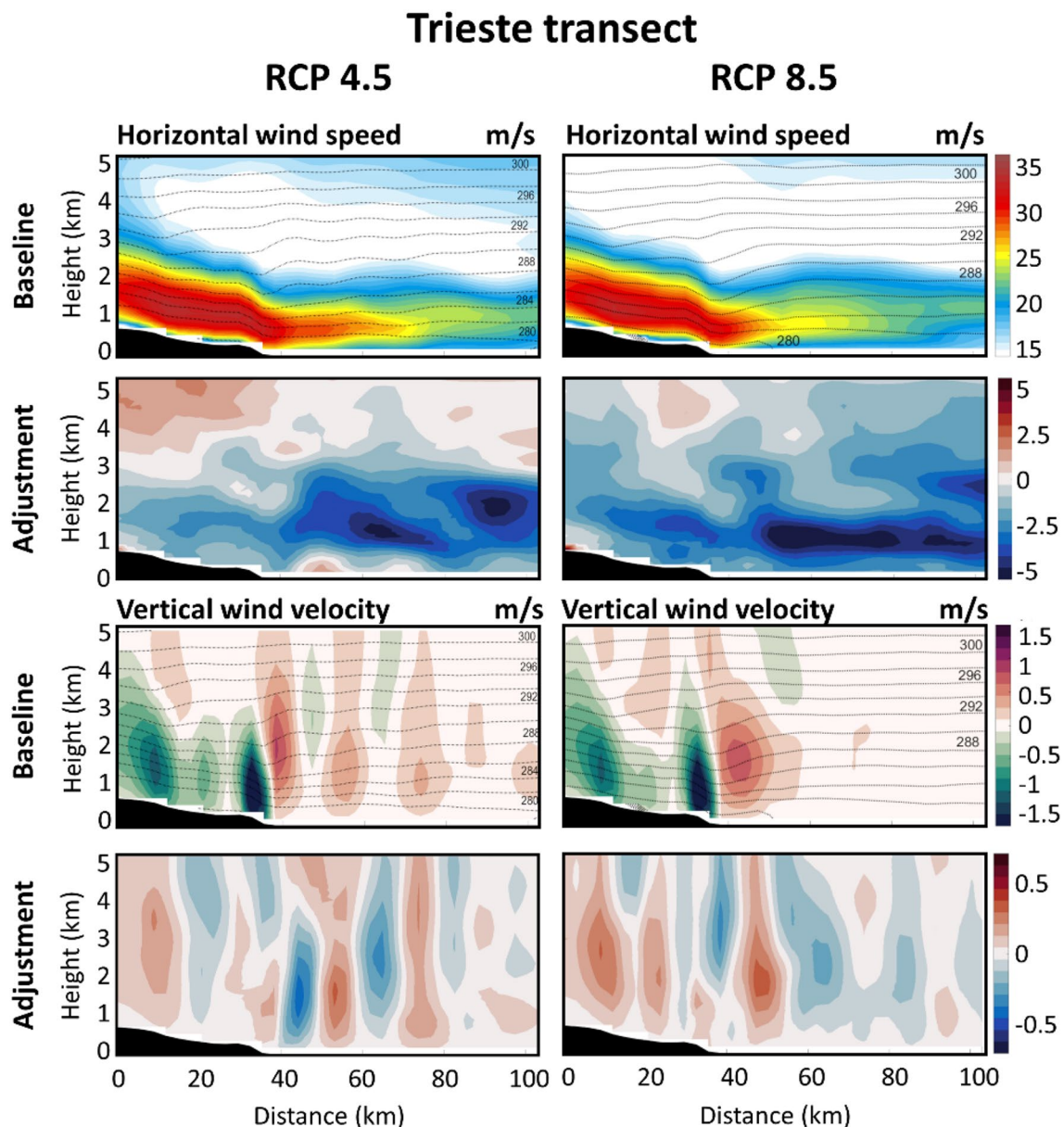


Fig. 4 Trieste cross-shore transect of baseline RCP 4.5 and RCP 8.5 conditions (median of the scenario results) and climate adjustment (median of difference between scenario and evaluation results) for

the horizontal wind speed, vertical wind velocity and virtual potential temperature (black isolines) during the peak of 22 selected extreme bora events

at surface). The associated climate adjustments are above 0.1 m/s along the lee of the Velebit mountain range, showing that atmospheric wave breaking is less intense under climate change and thus explaining the decrease of the wind speed intensity during bora events in future climate.

The vertical structures along the cross-shore transects (Figs. 4, 5, 6, 7 and 8) also present for both RCP 4.5 and RCP 8.5 scenarios the major known features of bora flows, even though, concerning the atmospheric rotors, the WRF 3-km model cannot properly represent the non-hydrostatic trapped lee-waves coexisting with bora-type hydraulic flows

(Zängl and Hornsteiner 2007; Gohm et al. 2008) and only can capture the hydraulic jump-like flow features (Grisogono and Belušić 2009; Prtenjak and Belušić 2009; Prtenjak et al. 2010). For all transects (Figs. 4, 5, 6 and 7), strong atmospheric wave breaking in the lee of the mountains—i.e. positive and negative vertical velocities with a magnitude above 1.5 m/s and sharp descent and re-ascent of the isentropes extending till 5 km of height—are present in both RCP 4.5 and RCP 8.5 scenarios. Yet, the associated climate adjustments—strongly positive (above 0.3 m/s and 0.5 m/s for RCP 4.5 and RCP 8.5 scenarios, respectively) where the

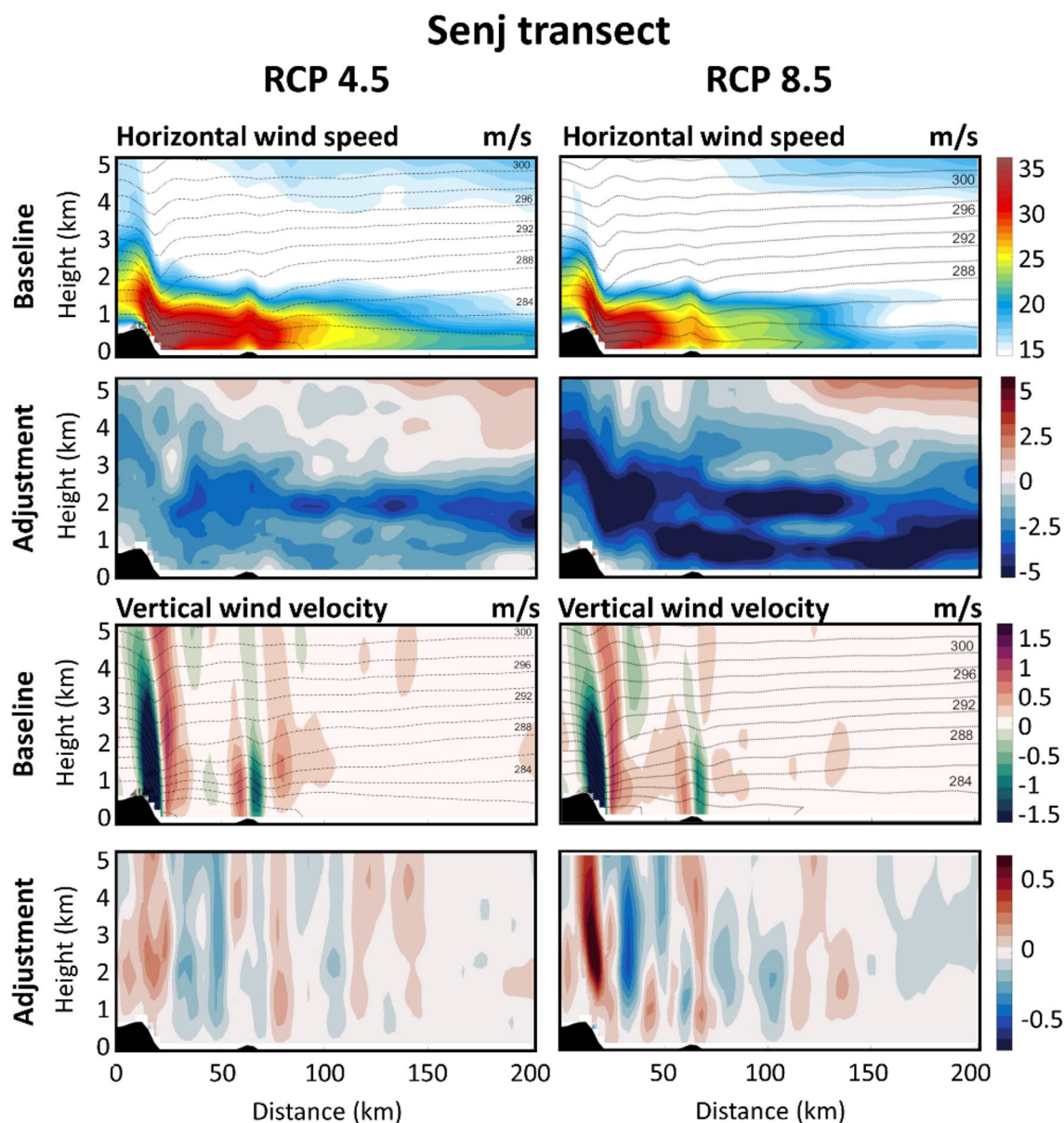


Fig. 5 Same as Fig. 4 but for the Senj cross-shore transect

vertical velocities are negative and vice versa—confirm that the atmospheric wave breaking is less intense in future climate projections than in evaluation mode as already seen in the surface plots (Fig. 2).

For the Trieste and Senj transects—located in mountain passes below 900 m, the RCP 4.5 and RCP 8.5 baseline conditions (Figs. 4 and 5) show a deep boundary layer flow with horizontal wind speed of 30 m/s which maintains its speed in the presence of a weak hydraulic jump (Figs. 8). The Froude number is always above 1, even though somewhat reduced -1.8 in Trieste and 1.2 in Senj near the surface on the lee side of the mountain. Additionally, the bora jets along these transects are strongly decelerated with climate

adjustments below -2.5 m/s and -5 m/s for RCP 4.5 and RCP 8.5 scenarios, respectively, up to 3 km above the surface. For the Zavižan and Gospić transects—crossing high mountain peaks (1100–1500 m), the RCP 4.5 and RCP 8.5 baseline conditions (Figs. 6 and 7) show a fast and thin boundary layer flow (horizontal velocities above 30 m/s near the surface and 0.5 km of height) associated with a strong near surface hydraulic jump (Fig. 8)—Froude number below 1 near the surface on the lee of the mountain. As for the Trieste and Senj transects, the bora jets are also strongly decelerated with climate adjustments up to -2.5 m/s and -5 m/s for RCP 4.5 and RCP 8.5 scenarios, respectively, but up to only 1.5 km above the surface. Furthermore, for

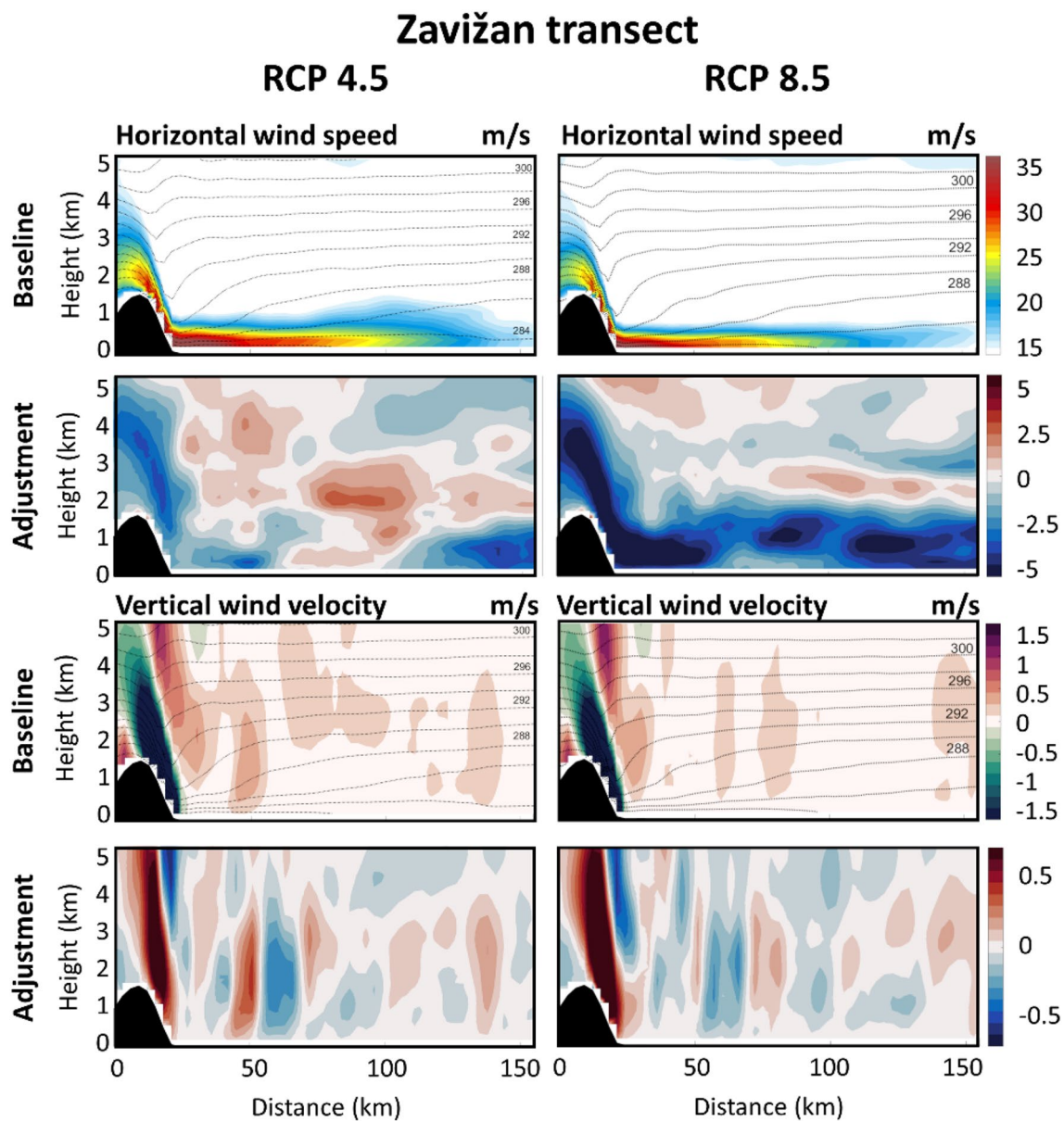


Fig. 6 Same as Fig. 4 but for the Zavižan cross-shore transect

both the Zavižan and the Gospić transects, horizontal wind speeds between 1.5 km and 3 km height are accelerated up to 2.5 m/s, mostly in the RCP 4.5 climate projections.

To summarize, the PGW climate projections for the 2060–2100 period (under RCP 4.5 and RCP 8.5 scenarios) of the ensemble of extreme bora events reveal that, despite a strong decrease in intensity of both the horizontal wind speeds as previously found in Belušić Vozila et al. (2019) and the atmospheric wave breaking along the lee of the Velebit mountain range (Figs. 2, 4, 5, 6 and 7), the main bora features—including jet and gap dynamics (Figs. 2 and 3), potential vorticity banners (Fig. 2) and hydraulic jumps (Fig. 8)—are expected to remain similar to the known bora

dynamics as described in details by Grisogono and Belušić (2009), even though far less energetic.

3.2 Impact of climate change on sea surface cooling

Over the northern Adriatic Sea where the densest water in the Mediterranean Sea are formed, the bora jets not only drive the westward offshore circulation leading to coastal downwelling along the Italian coastline (Kourafalou 1999), but also generate intense air–sea interactions increasing the net upward sea surface heat fluxes and thus inducing negative buoyancy fluxes associated with sea surface cooling (e.g. Zore-Armanda and Gačić 1987; Paklar et al. 2001;

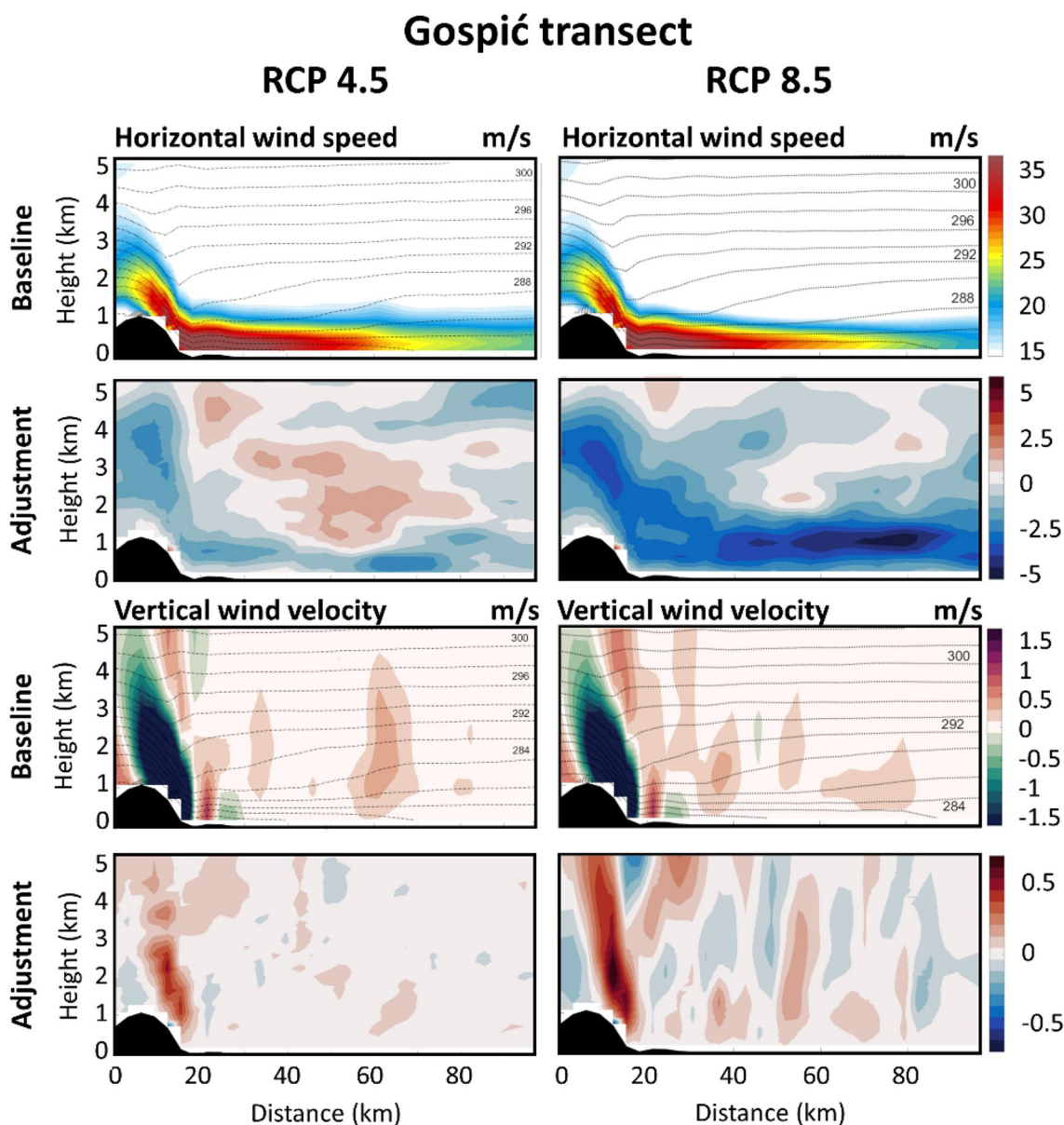


Fig. 7 Same as Fig. 4 but for the Gospić cross-shore transect

Raichich et al. 2013; Janeković et al. 2014; Ličer et al. 2016; Vilibić et al. 2016, 2018). To better understand the impact of climate change on sea surface cooling during extreme bora events projected for the 2060–2100 period, the total heat flux (positive downward and negative for heat loss)—including long-wave and short-wave radiations as well as sensible and latent heat flux (see Appendix for more details)—and the sea surface temperature (SST) anomaly (negative for sea surface cooling) are presented for RCP 4.5 and RCP 8.5 scenarios as: (1) minimum (Fig. 9) baseline conditions (i.e. median over the ensemble of minimum values for each event) and climate adjustments (i.e. median of the difference between scenario and evaluation minimum conditions),

and (2) probability distribution functions (PDFs) for the ensemble of hourly results (Fig. 10) at 12 locations (Fig. 1, points P1–P12) where the most intense sea surface cooling is occurring.

Spatially, the known bora air–sea interactions can still clearly be seen in the RCP 4.5 and RCP 8.5 baseline conditions derived from the WRF 3-km and ROMS 1-km simulations (Fig. 9). The largest total heat losses (i.e. the most negative total heat fluxes) are still found along the bora jets—in particular following the Trieste, Senj, Zavižan and Gospić transects with median values above 550 W/m^2 . The largest sea surface cooling areas (i.e. negative SST anomalies) are found (1) along the Italian coastline where the sea

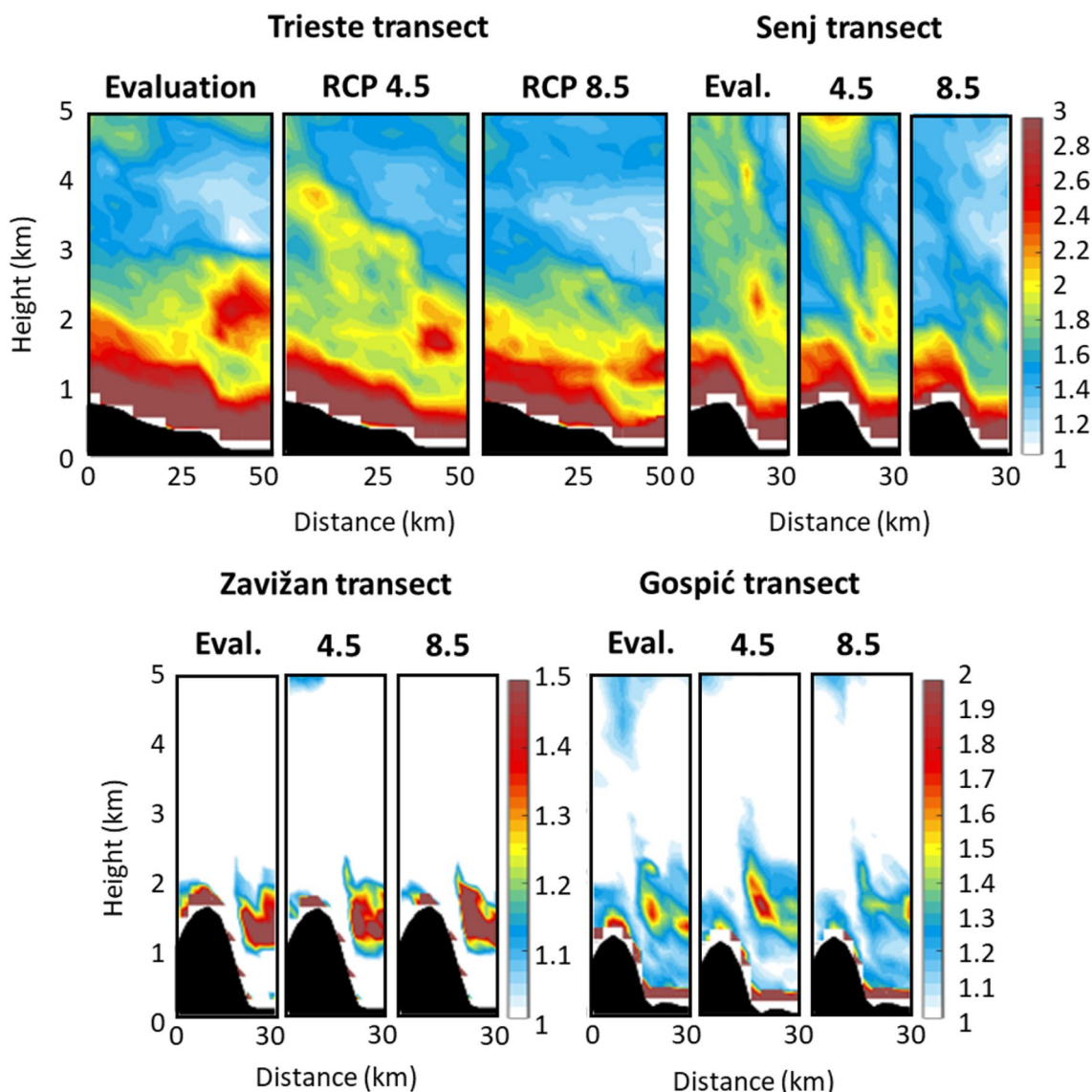


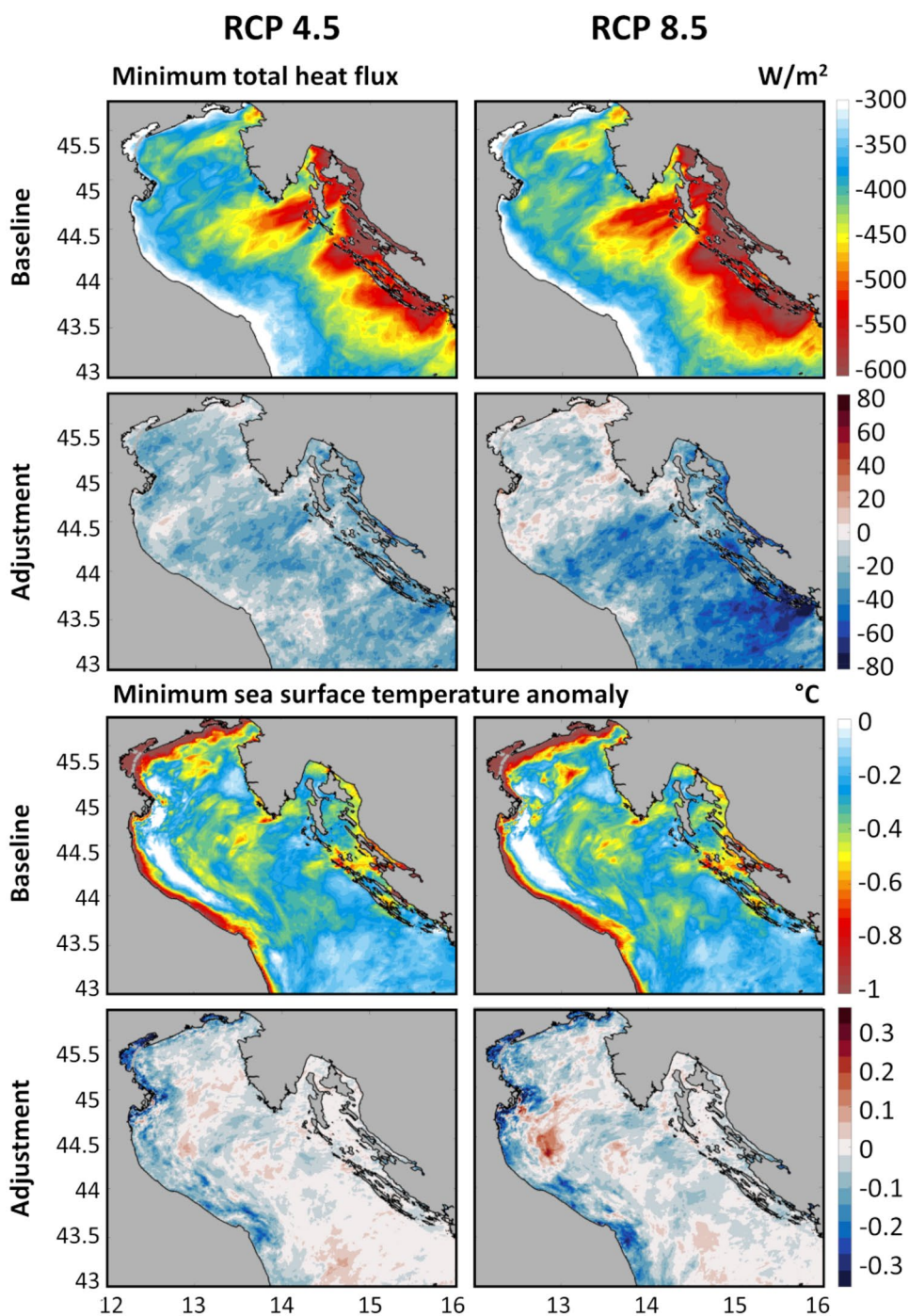
Fig. 8 Froude number derived for the evaluation (Eval.) as well as RCP 4.5 (4.5) and RCP 8.5 (8.5) scenario simulations, near the mountain peaks of the Trieste, Senj, Zavižan and Gospić transects

is quite shallow, thus prone to intense cooling, and strongly influenced by rivers (more than 1 °C for both scenarios), (2) within the Kvarner Bay coastal area (above 0.5 °C and 0.6 °C for RCP 4.5 and RCP 8.5 scenarios, respectively) and (3) within the open northern Adriatic shallow shelf (above 0.6 °C and 0.7 °C for RCP 4.5 and RCP 8.5 scenarios, respectively). Additionally, for both future climate projections, the total heat losses increase along the bora jets—climate adjustments of the total heat flux reaching -40 W/m^2 and -60 W/m^2 for RCP 4.5 and RCP 8.5 scenarios respectively—except along the Trieste transect where the climate adjustments reach 10 W/m^2 for the RCP 8.5 scenario. Surprisingly, this spatial analysis of the climate adjustments during extreme bora events, showing an increase in total

heat losses, might look in contradiction with the substantial decrease in intensity of the bora winds forecasted in future climates (Fig. 3). These surprising results will thus be further analyzed in this study. Additionally, concerning the sea surface cooling (Fig. 9), the impact of climate change seems inconclusive for both RCP 4.5 and RCP 8.5 projections, with SST climate adjustments varying between -0.2 and 0.2 °C , over the entire domain.

In line with the spatial analysis, PDFs of hourly total heat fluxes and SST anomalies at locations P1–P12 (Fig. 10) confirm that, under both RCP 4.5 and RCP 8.5 scenarios, the total heat losses are likely to increase. Further, the distributions of the future sea surface cooling are overall likely to be similar to the evaluation mode. In more details, the sea

Fig. 9 Baseline RCP 4.5 and RCP 8.5 conditions (median of the scenario results) and climate adjustment (median of difference between scenario and evaluation results) for the minimum of both the total heat flux and the sea surface temperature anomaly during each of the 22 selected events



surface cooling is clearly likely to decrease at points P1, P2 and P4 and to increase at points P6, P7 and P12, while for the other points the impact of climate change is most likely to vary from event to event. The change in SST anomaly PDFs between RCP 4.5 and RCP 8.5 scenario and evaluation modes, as may be notably noticed at points P1 and P4, identify the ocean regions where hourly SST changes are not only driven by the bora-driven cooling, but also by other bora-driven ocean processes acting on hourly timescale such

as the fluctuations of the thermohaline front normally present in the northern Adriatic (Jeffries and Lee 2007; Kokkini et al. 2017) and the local upwelling and downwelling due to horizontal shear in regions with strong bora-driven currents—e.g. along the Senj jet (Kuzmić et al. 2007).

The PDF analysis (Fig. 10) thus confirms the findings of the spatial analysis (Fig. 9) and raised two important questions: (1) how well the sea surface cooling is correlated to the heat losses, and (2) how these heat losses can

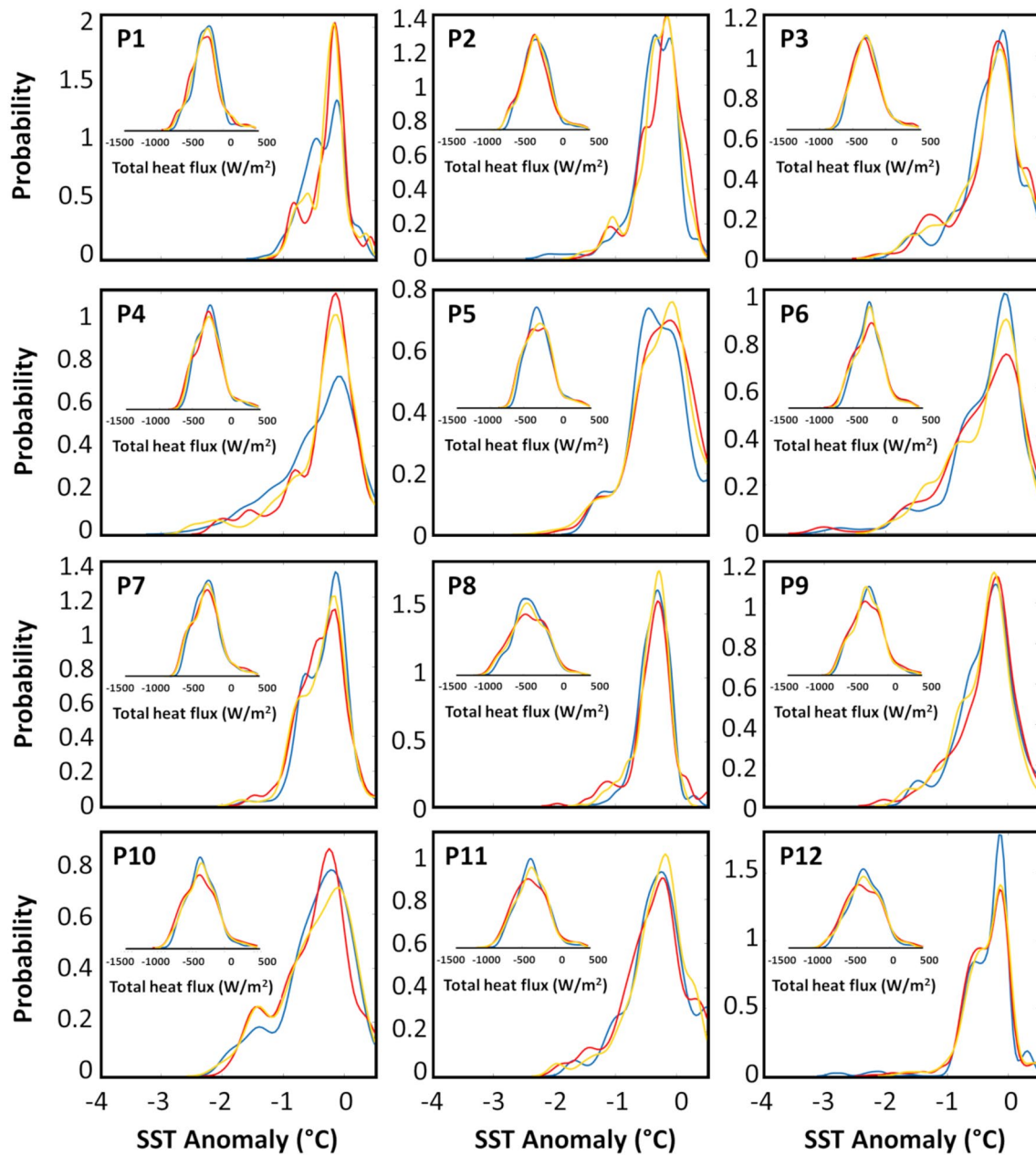


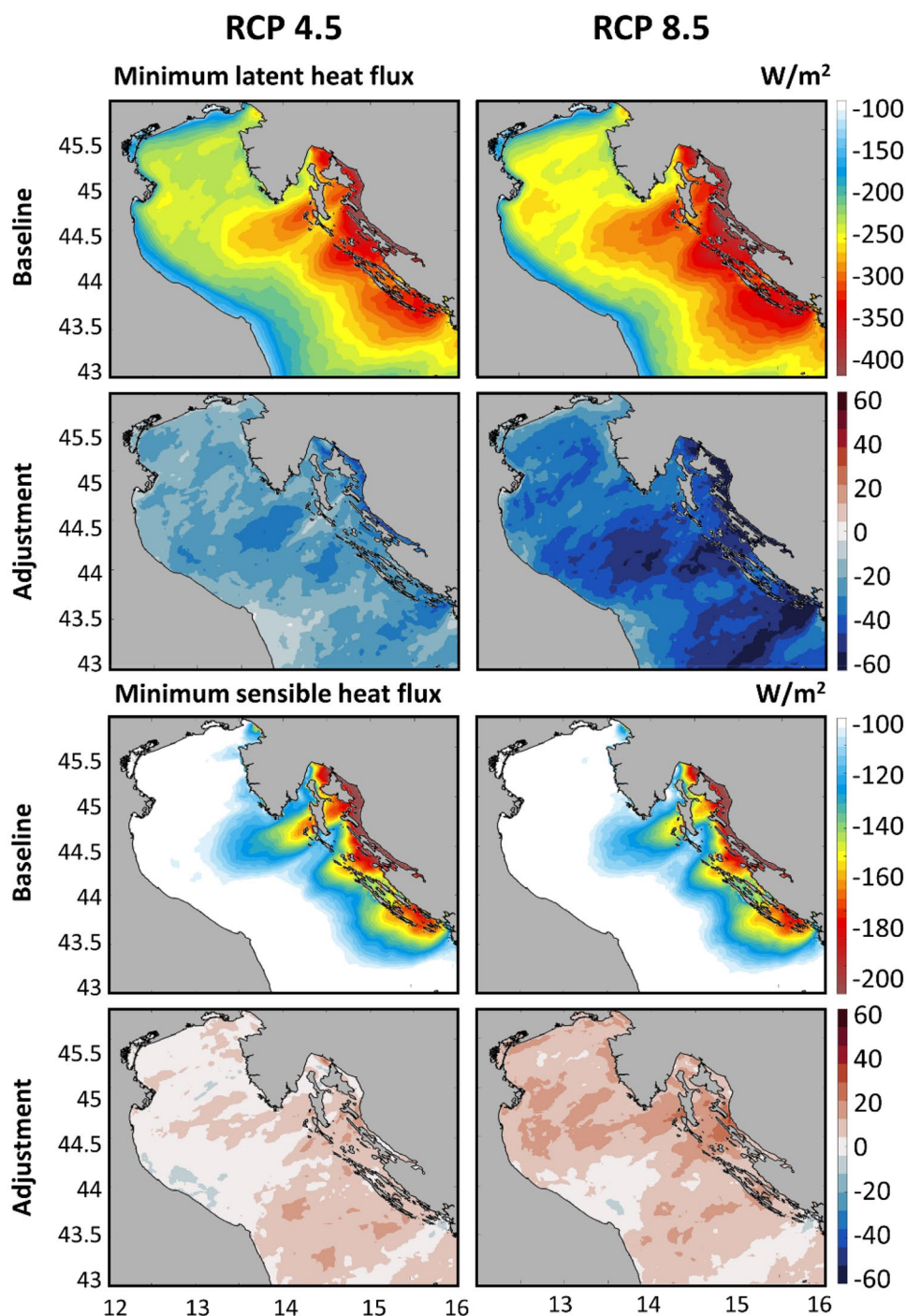
Fig. 10 Probability density functions of the hourly evaluation (in blue), RCP 4.5 (in orange) and RCP 8.5 (in red) total heat fluxes and the sea surface temperature (SST) anomalies for the ensemble of the 22 selected event results at locations P1 to P12

increase under climate change while the intensity of the wind decreases?

To answer the first question, the total heat flux is first decomposed into radiations (including long- and short-waves), latent heat flux and sensible heat flux. As the impact of radiations on sea surface cooling is known to be negligible during extreme bora events, only the RCP 4.5 and RCP 8.5 baseline conditions and climate adjustments of the sensible and latent heat fluxes are analyzed hereafter (Fig. 11). The RCP 4.5 and RCP 8.5 baseline conditions reveal that

latent heat losses (with the respective values reaching up to 350 W/m^2 and 400 W/m^2) are twice as strong as sensible heat losses (reaching up to 200 W/m^2) along the main bora jets. Furthermore, and even more interestingly, the RCP 4.5 and RCP 8.5 climate adjustments show a homogeneous increase of the latent heat losses reaching up to 35 W/m^2 and 60 W/m^2 respectively, and a nearly homogeneous decrease of the sensible heat losses reaching -15 W/m^2 and -20 W/m^2 respectively (as expected with the decrease of the bora wind speeds). Finally, the spatial correlations of

Fig. 11 Baseline RCP 4.5 and RCP 8.5 conditions (median of the scenario results) and climate adjustment (median of difference between scenario and evaluation results) for the minimum of both the latent heat flux and the sensible heat flux during each of the 22 selected events



the SST anomalies with the total, sensible and latent heat fluxes in both evaluation and climate projection (for RCP 4.5 and RCP 8.5 scenarios) modes are presented Fig. 12. To be noted, the white areas representing insignificant correlations are located where the bora-driven ocean dynamics is expected to be the strongest: (1) in the vicinity of the Po river delta, where the freshened coastal waters of different temperature are advected off the coast through a cyclonic gyre (Zore-Armanda and Gačić 1987; Paklar et al. 2001;

Kuzmić et al. 2007), (2) along the western Adriatic coast influenced by the Po river waters, where the western coastal current of waters with lower salinity and different temperature is normally intensified and becomes laminar during bora events (Vilibić et al. 2009), and (3) along the Senj transect where the Kvarner Bay waters are transported towards the northern Adriatic shelf and generate a thermohaline front that may fluctuate (Kokkini et al. 2017).

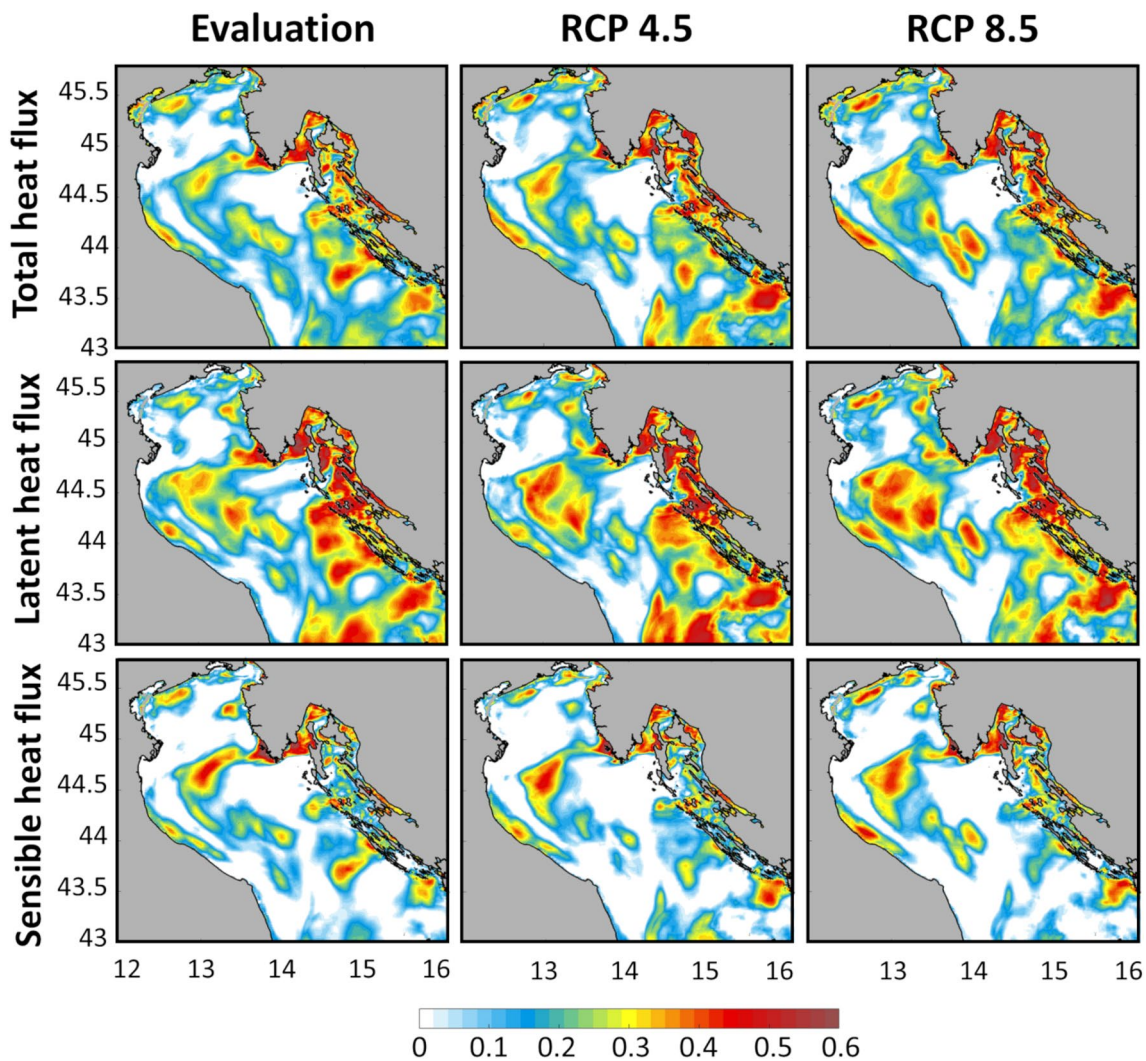


Fig. 12 Spatial variations of the Pearson’s correlation coefficients calculated between the hourly sea surface temperature and the hourly total, sensible and latent heat fluxes for the evaluation, RCP 4.5 and

RCP 8.5 results of the 22 selected extreme bora events. The areas where the correlation is insignificant (following the null hypothesis of the t test) are represented in white

However, the analysis clearly shows that the highest correlations over the entire northern Adriatic domain are found for the latent heat fluxes and tend to slightly increase in the middle of the shelf under RCP 4.5 and RCP 8.5 scenarios. Consequently, the increase in latent heat losses under climate change projections is driving the sea surface cooling during extreme bora events, and therefore may influence the dense water formation and the thermohaline circulation in the area. A thorough analysis of the latent heat flux is thus performed further in this study.

To answer the second question and understand the increase in latent heat losses despite the decrease of the bora wind speeds under climate projections, a full diagnosis of the different physical quantities (i.e. relative humidity and air–sea saturation specific humidity, see definitions in [Appendix](#)) used to derive these fluxes is performed for

the RCP 8.5 scenario only (Fig. 13). Along the bora jets in the northern Adriatic Sea, the baseline relative humidity (between 85 and 90%) is expected to decrease under RCP 8.5 climate projections as it is associated with nearly homogeneous negative climate adjustments reaching -3% (except along the Trieste transect where values are positive and reach up to 2%). The increase of the saturation specific humidity (SAT)—associated with positive climate adjustments due to the projected increase in temperatures—is consequently lower in the air (1.5 g/kg), as compensated by the decrease in relative humidity, than over the sea (2.5 g/kg on average). As a final result, the air–sea SAT differences driving the latent heat losses is much lower (below -4.5 g/kg) for the RCP 8.5 scenario than for the evaluation conditions (-3.5 g/kg on average). Under the RCP 4.5 and RCP 8.5 climate changes used in this study, the decrease of

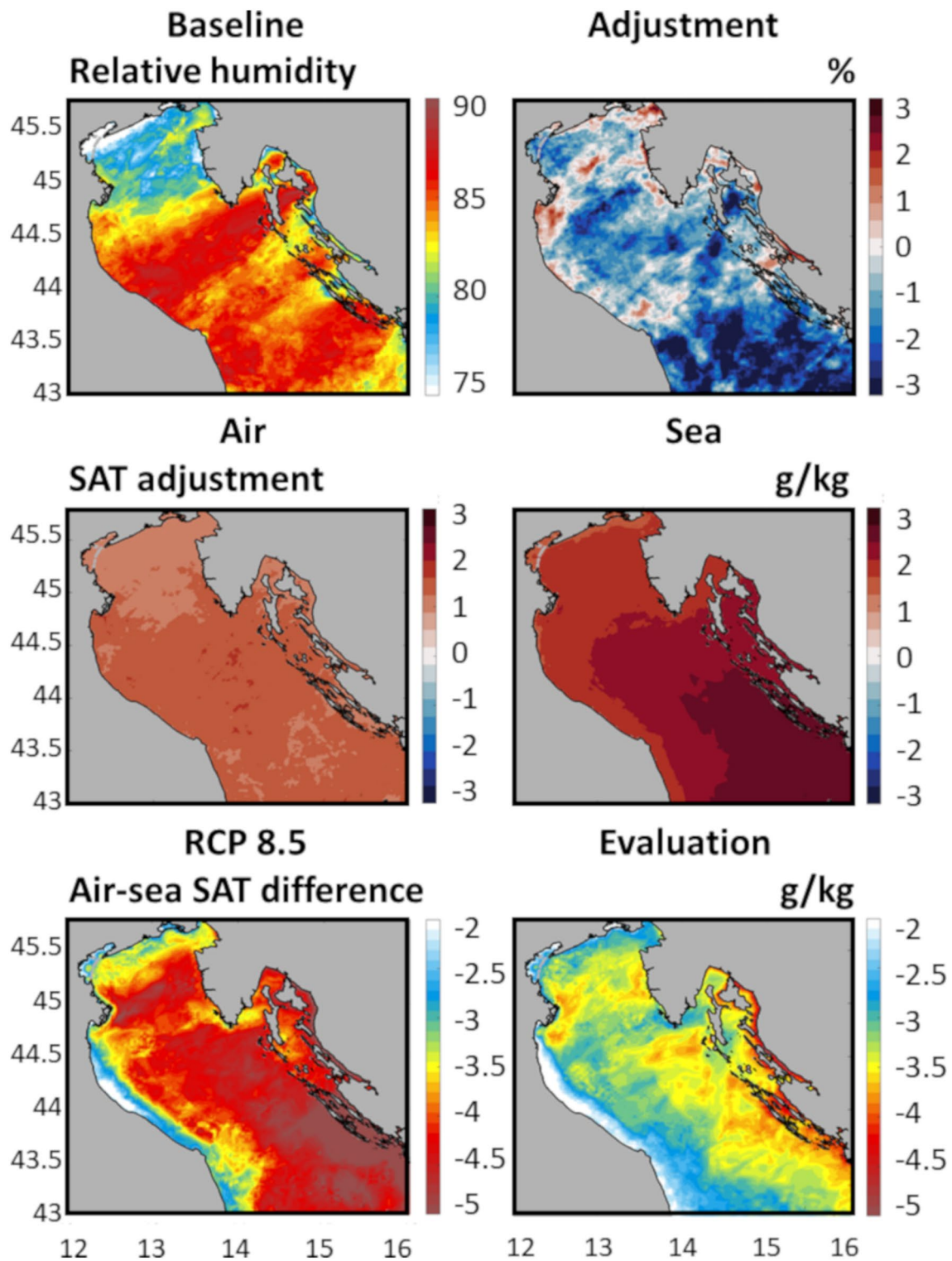


Fig. 13 RCP 8.5 baseline and climate adjustment conditions of the relative humidity at 2 m (top panels), RCP 8.5 climate adjustment conditions of 2 m air and sea surface saturation specific humidity

(SAT) (middle panels) and median, over the ensemble of 22 selected events, of the air–sea saturation specific humidity (SAT) difference for both RCP 8.5 and evaluation modes (bottom panels)

relative humidity during extreme bora events is thus key to the increase in latent heat losses driving the future sea surface cooling in the northern Adriatic Sea, which is likely to be as strong as in the evaluation mode, despite the projected sharp decrease in wind speeds.

Lastly, in order to better understand the interconnections between latent heat losses and sea surface cooling, the joint probability distributions of latent heat fluxes and SST anomalies, in evaluation and scenario (RCP 4.5 and RCP 8.5) modes, are analyzed for points P1–P12 (Figs. 14 and 15). Overall, as expected due to the somewhat weak

correlation between the two physical quantities (Fig. 12), no linear behavior can be derived from the joint probabilities even though, along the northern Croatian coastline for points P7–P12 (Fig. 15)—at locations where the Pearson’s correlation coefficient reaches up to 0.6—the linear relationship seems stronger than in the middle of the northern Adriatic shelf (P1–P6). However, for all the points compared to the evaluation results, the higher probabilities are shifted towards the largest latent heat losses by about 40 W/m² in RCP 4.5 scenario and 70 W/m² in RCP 8.5 scenario for mild sea surface cooling (below 1 °C), and by 100 W/

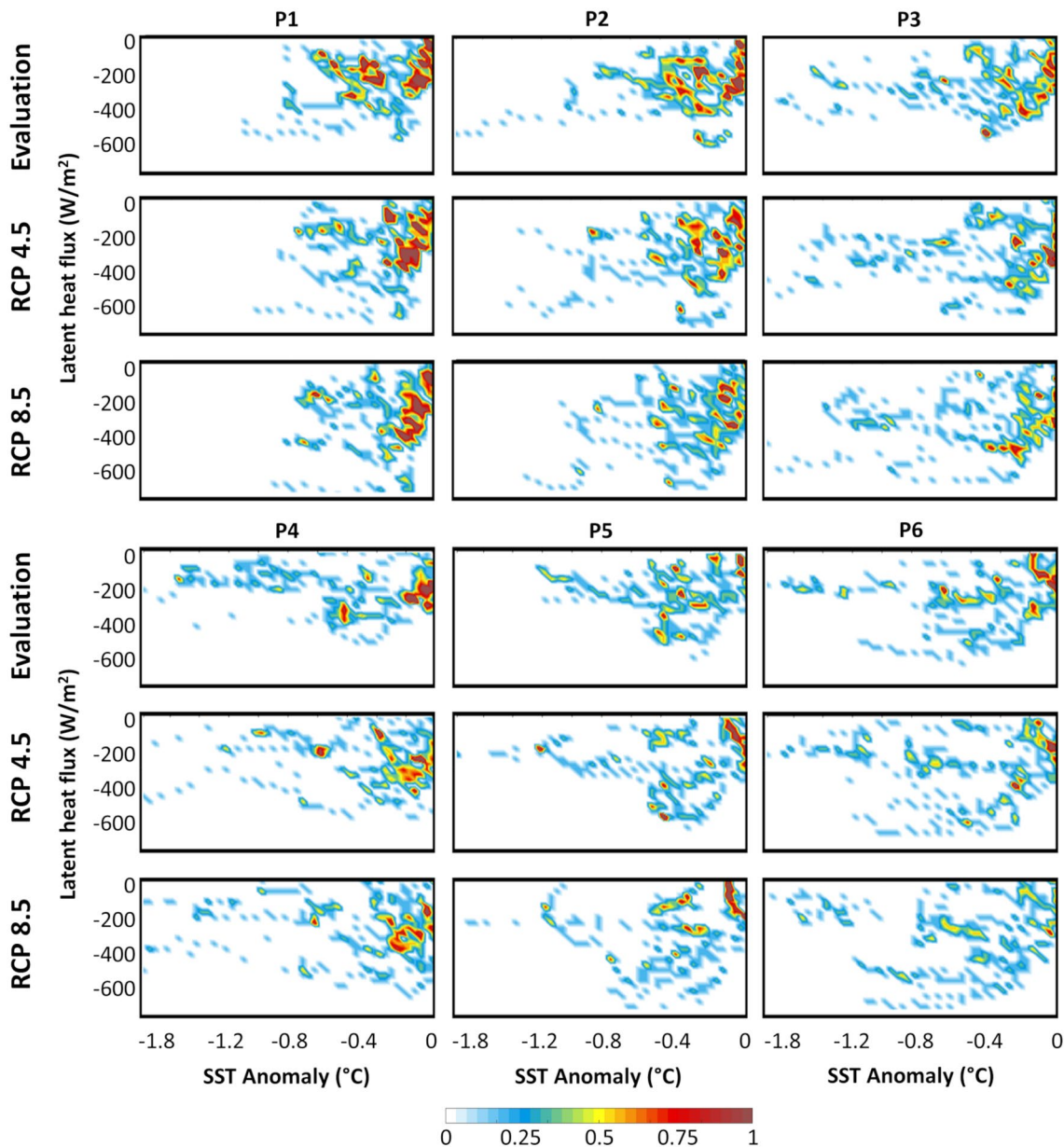


Fig. 14 Joint probability distributions (in percent) derived at points P1–P6 from the hourly surface latent heat fluxes (between – 800 and 0 W/m²) and the SST anomalies (between – 2 and 0 °C) defined for

the ensemble of 22 events in both evaluation and scenario (RCP 4.5 and RCP 8.5) modes

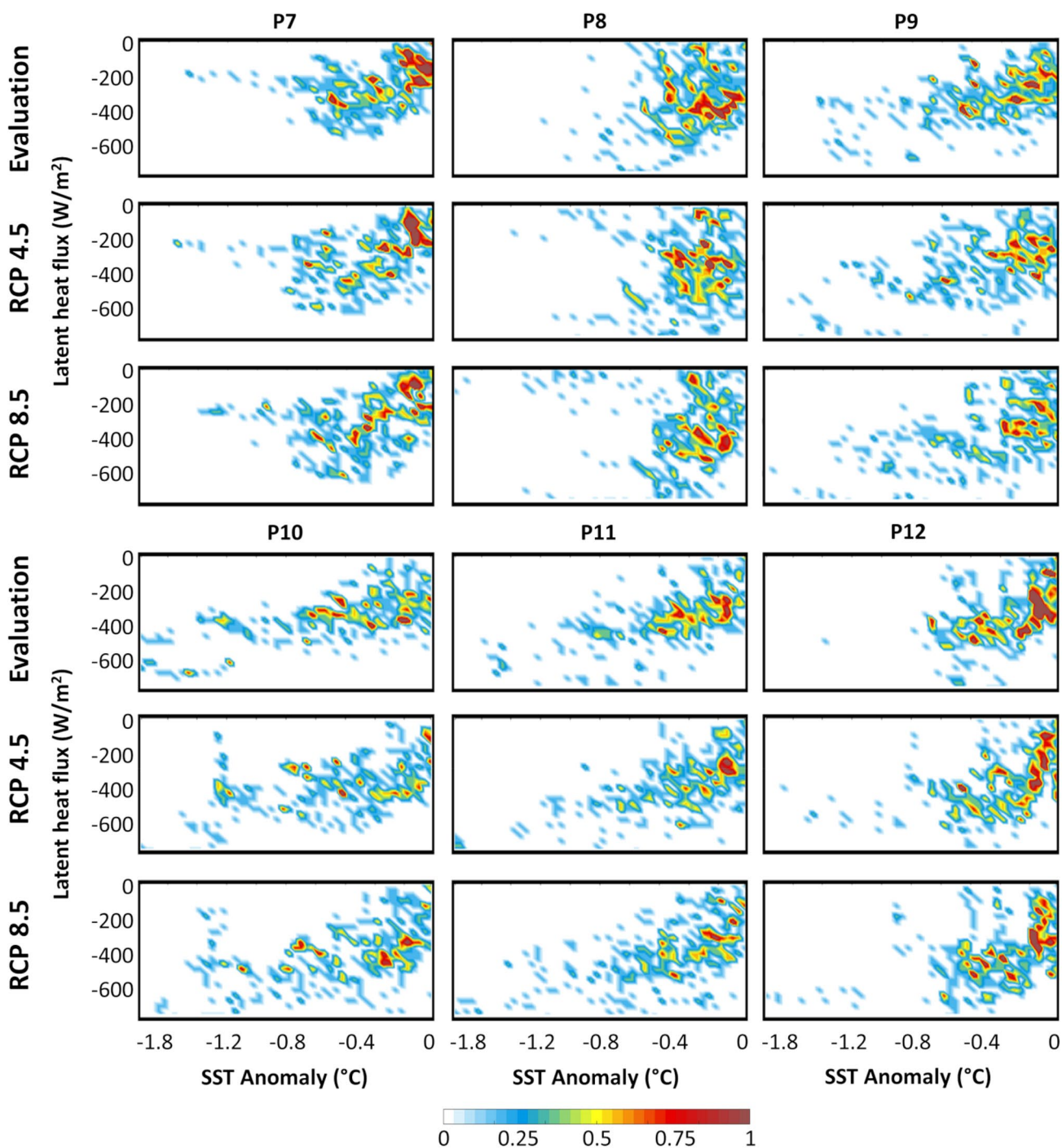


Fig. 15 Joint probability distributions (in percent) derived at points P7–P12 from the hourly surface latent heat fluxes (between -800 and 0 W/m^2) and the SST anomalies (between -2 and $0 \text{ }^\circ\text{C}$) defined

for the ensemble of 22 events in both evaluation and scenario (RCP 4.5 and RCP 8.5) modes

m^2 in RCP 4.5 scenario and 150 W/m^2 in RCP 8.5 scenario for intense sea surface cooling (above $1.75 \text{ }^\circ\text{C}$). In other words, the latent heat losses needed to cool by $1 \text{ }^\circ\text{C}$ the sea surface water under global warming are increased by $40\text{--}100 \text{ W/m}^2$ for RCP 4.5 scenario and by $70\text{--}150 \text{ W/m}^2$

for RCP 8.5 scenario compared to the evaluation mode. To better quantify this shift in intensity of the latent heat losses needed to cool the sea surface, three probabilities are extracted from the joint probability distributions at locations P1–P12 and presented in Table 2: probability in

Table 2 Probabilities (in percent) derived from the joint probability distributions at points P1–P12 of the hourly surface latent heat fluxes and the SST anomalies defined for the ensemble of 22 events in both evaluation and scenario (RCP 4.5 and RCP 8.5) modes

	Probability (%) of latent heat flux below -400 W/m^2 and negative SST anomaly			Probability (%) of latent heat flux below -400 W/m^2 and SST anomaly below $-1 \text{ }^\circ\text{C}$			Probability (%) of negative latent heat flux and SST anomaly below $-1 \text{ }^\circ\text{C}$		
	Evaluation	RCP 4.5	RCP 8.5	Evaluation	RCP 4.5	RCP 8.5	Evaluation	RCP 4.5	RCP 8.5
P1	0.0	3.3	4.2	0.0	2.9	3.9	2.1	0.8	0.6
P2	1.1	4.7	5.3	1.1	3.6	3.6	3.5	5.5	4.4
P3	0.0	2.3	2.7	0.0	2.3	2.0	6.4	9.2	10.0
P4	0.0	0.0	1.2	0.0	0.0	1.2	12.0	6.2	7.1
P5	0.2	0.3	3.0	0.2	0.3	3.0	5.2	5.8	5.5
P6	0.5	4.4	4.7	0.5	3.5	3.8	7.4	11.2	9.2
P7	0.0	0.8	2.6	0.0	0.8	2.6	1.8	2.4	3.5
P8	4.4	10.5	12.7	4.1	8.5	10.3	1.1	3.5	5.9
P9	2.4	3.3	5.0	0.9	0.9	2.7	6.2	7.6	7.6
P10	3.6	4.8	8.6	0.0	1.2	3.2	11.7	13.2	13.5
P11	3.5	7.0	9.4	1.7	3.5	5.2	7.1	6.2	8.0
P12	3.9	6.5	11.1	3.9	5.9	9.5	0.2	2.6	2.7

percent of latent heat flux below -400 W/m^2 for negative SST anomalies $\Pr(Q_E \leq -400 \text{ W/m}^2 \cap \Delta\text{SST} \leq 0^\circ\text{C})$, probability in percent of negative latent heat flux for SST anomaly below $-1 \text{ }^\circ\text{C}$ $\Pr(Q_E \leq 0 \text{ W/m}^2 \cap \Delta\text{SST} \leq -1^\circ\text{C})$, as well as probability in percent of latent heat flux below -400 W/m^2 for SST anomaly below $-1 \text{ }^\circ\text{C}$ $\Pr(Q_E \leq -400 \text{ W/m}^2 \cap \Delta\text{SST} \leq -1^\circ\text{C})$.

In average and for all the locations, the probabilities in scenario modes are always higher than in evaluation mode:

- (1) By 2.4% and 4.2% for RCP 4.5 and RCP 8.5 scenarios, respectively, concerning $\Pr(Q_E \leq -400 \text{ W/m}^2 \cap \Delta\text{SST} \leq 0^\circ\text{C})$ —all sea surface cooling are thus more likely to require latent heat losses above 400 W/m^2 in scenario modes (particularly in RCP 8.5 scenario) than in evaluation mode;
- (2) By 0.8% and 1.1% for RCP 4.5 and RCP 8.5 scenarios, respectively, concerning $\Pr(Q_E \leq 0 \text{ W/m}^2 \cap \Delta\text{SST} \leq -1^\circ\text{C})$ —sea surface cooling above $1 \text{ }^\circ\text{C}$ is thus, in average, slightly more likely to occur in scenario modes than in evaluation mode;
- (3) And by 1.8% and 3.2% for RCP 4.5 and RCP 8.5 scenarios, respectively, concerning $\Pr(Q_E \leq -400 \text{ W/m}^2 \cap \Delta\text{SST} \leq -1^\circ\text{C})$ —following the two previous results, sea surface cooling above $1 \text{ }^\circ\text{C}$ associated with latent heat losses above 400 W/m^2 are thus more likely to happen in scenario modes (particularly in RCP 8.5 scenario) than in evaluation mode.

Additionally, for all three probabilities, the minimum and maximum changes between scenario and evaluation modes are found for locations P4 and P8 at the end and the beginning of the Senj transect respectively, with values of:

- (1) 0% at P4, 6.1% at P8 for RCP 4.5 scenario and 1.2% at P4, 8.3% at P8 for RCP 8.5 scenario concerning $\Pr(Q_E \leq -400 \text{ W/m}^2 \cap \Delta\text{SST} \leq 0^\circ\text{C})$ —along the Senj transect, sea surface cooling is thus likely to require much higher latent heat losses (above 400 W/m^2) at the beginning of the transect, within the Kvarner Bay, in scenario modes than in evaluation modes but nearly no latent heat losses above 400 W/m^2 at the end of the transect for all the modes (0% in both evaluation and RCP 4.5 modes and 1.2% in RCP 8.5 mode);
- (2) -5.8% at P4, 2.4% at P8 for RCP 4.5 and -4.9% at P4, 4.8% at P8 for RCP 8.5 scenario concerning $\Pr(Q_E \leq 0 \text{ W/m}^2 \cap \Delta\text{SST} \leq -1^\circ\text{C})$ —in a warmer future, sea surface cooling above $1 \text{ }^\circ\text{C}$ is likely to increase at the beginning of the Senj transect (by 2.4% and 4.8% in RCP 4.5 and RCP 8.5 modes respectively) but largely decrease at the end of the transect (by about -5% for both scenario modes) in the middle of the northern Adriatic shelf;
- (3) 0% at P4, 4.4% at P8 for RCP 4.5 scenario and 1.2% at P4, 6.2% at P8 for RCP 8.5 scenario concerning $\Pr(Q_E \leq -400 \text{ W/m}^2 \cap \Delta\text{SST} \leq -1^\circ\text{C})$ —following the two previous results, sea surface cooling above $1 \text{ }^\circ\text{C}$ associated with latent heat losses above 400 W/m^2 is thus likely to strongly increase at the beginning of the Senj transect (up to 6.2% for RCP 8.5 scenario) but remain identical at the end of the transect in a warmer climate.

Finally, the highest probabilities of extreme sea surface cooling $\Pr(Q_E \leq 0 \text{ W/m}^2 \cap \Delta\text{SST} \leq -1^\circ\text{C})$, are found for locations P10 in the Kvarner Bay near the Zavižan transect (11.7% in evaluation mode, 13.2% and 13.5% in RCP 4.5 and RCP 8.5 scenario modes), P4 at the end of the Senj transect

(12% in evaluation mode), P6 at the end of the Trieste transect (11.2% in RCP 4.5 mode) and P3 in the middle of the northern Adriatic shelf near the Senj transect (10% in RCP 8.5 mode).

In a nutshell, despite the expected sharp decrease in intensity of the severe bora wind speeds in a warmer climate under RCP 4.5 or RCP 8.5 scenarios for the 2060–2100 period, the sea surface cooling in the northern Adriatic Sea—preconditioning the formation of the densest waters in the Mediterranean Sea and mostly impacted by the latent heat losses, is expected to remain identical or even to slightly increase for values above 1 °C. This can be explained by the increase of the latent heat losses resulting from the forecasted decrease in relative humidity in the PGW climate simulations. Additionally, the maximum changes (between scenario and evaluation modes) in both sea surface cooling and latent heat losses are expected to occur along the Senj transect, where historically the strongest bora winds are blowing. Finally, the locations of the extreme sea surface cooling is likely to change in the future, except maybe in the vicinity of point P10 in the Kvarner Bay near the Zavižan transect.

4 Discussion and conclusions

Due to the tremendous computational cost of coupled kilometer-scale models, climate studies in the Mediterranean and Adriatic seas have been carried out with regional climate models with resolutions of the order of 10 km. However, although many important features of the general atmosphere–ocean circulation are captured with such models, they often reach their limits during extreme events in coastal areas where both the orography and the geomorphology strongly influence the intensity of the storms (Vosper et al. 2018). This is particularly true in the Adriatic Sea during severe bora events, where several studies have demonstrated that bora dynamics can only be captured with limited area atmospheric models (Grisogono and Belušić 2009; Trošić and Trošić 2010; Prtenjak et al. 2010; Kuzmić et al. 2015; Josipović et al. 2018; Belušić Vozila et al. 2019; Denamiel et al. 2020).

Despite the known numerical cost and slowness of the AdriSC climate model with resolutions of 3-km in the atmosphere and 1-km in the ocean (Denamiel et al. 2019, 2020), the conjoint use of an ensemble approach and the pseudo-global warming (PGW) methodology for short-term simulations (i.e. 3 days) allowed to both accurately represent historical bora storms and, in this study, better understand the impact of global warming on extreme bora dynamics and sea surface cooling in the northern Adriatic region (under both RCP 4.5 and RCP 8.5 scenarios). This has been achieved using far less computational resources

than a traditional regional climate model running 30 years in evaluation mode, 50 years in historical mode and 100 years in scenario mode. Such a method has nevertheless some intrinsic limitations, including (1) the use of a relatively small ensemble of 22 storms which may not be fully representative of neither the historical Adriatic extreme bora events nor their future projections for the 2060–2100 period, (2) the shortness of the simulations carried over a three-day period which increases the influence of the imposed initial conditions on the analyzed results compared to long-term simulations, (3) the use of the same ensemble of storms in evaluation and climate projection modes which prevents the forecast of the extreme event frequency under climate change and finally, and (4) the derivation of the PGW forcing from a single model instead of an ensemble of regional climate models which would have provide more robust climate change projections.

Notwithstanding these limitations, the statistical approach presented in this study—consisting in running ensembles of short simulations for extreme events, has provided some new insights in terms of the future of the bora dynamics and sea surface cooling for the 2060–2100 period under both RCP 4.5 and RCP 8.5 scenarios:

- The sharp decrease in intensity of the bora horizontal wind speeds between the surface and 2 km of height—also seen, to some extent, by the EURO-CORDEX ensemble (Belušić Vozila et al. 2019), is mostly due to the strong decrease in intensity of the atmospheric wave breaking along the lee of the Velebit mountain range which is generally not well captured by regional climate models (Josipović et al. 2018);
- The other known bora features—only seen with kilometer-scale atmospheric models as driven by the complex orography and consisting in jet and gap dynamics, potential vorticity banners and hydraulic jumps—are expected to remain preserved in a warmer climate;
- Due to the decrease in relative humidity, the latent heat losses, driving the sea surface cooling in the northern Adriatic Sea, are expected to increase under global warming despite the decrease of the bora wind speeds;
- The extreme sea surface cooling (above 1 °C) is expected, on the one hand, to require larger latent heat losses (due to the presence of warmer waters) and, on the other hand, to remain identical or even to slightly increase in the future, even though not necessarily at the same locations than in evaluation mode.

Following the results presented in this study, for a future warmer climate, due to an increase in latent heat losses driven mostly by a decrease in relative humidity, the rates of dense water formation might remain untouched which might have important consequences concerning the

thermohaline circulation in the Adriatic-Ionian region. In particular it may influence the future of the decadal oscillations of the Adriatic thermohaline and biogeochemical properties driven by the Adriatic-Ionian Bimodal Oscillating System (BiOS, Gačić et al. 2010; Civitarese et al. 2010; Vilibić et al. 2012; Batistić et al. 2014), the ventilation of deep Adriatic and Eastern Mediterranean waters (Powley et al. 2016; de Ruggiero et al. 2018), the open-ocean convection in the southern Adriatic (Gačić et al. 2002) and the anoxic conditions in the northern and middle Adriatic as well as the associated impact to the benthic organisms (Krasakopoulou et al. 2005; Blasnig et al. 2013). The findings of this study may also be relevant to other dense water formation areas (e.g. Ivanov et al. 2004) and other coastal areas substantially influenced by the orography, for which climate change assessment requires kilometre-scale simulations.

As the increase of both air–sea flux intensity and sea surface cooling during future extreme bora events is not aligned with previous findings from Soto-Navarro et al. (2020) who analyzed the results of the Med-CORDEX ensemble, more research is needed to confirm the validity of these findings. In particular, the analysis of the 31-year long AdriSC climate simulations in both evaluation and RCP 8.5 scenario modes will provide, in a near future, more robust results concerning the sea surface cooling but also the dense water formation in the northern Adriatic shelf. In addition, the sensitivity of the AdriSC model RCP 4.5 and RCP 8.5 projections to the PGW forcing should also be investigated in order to increase the confidence in the results presented in this study.

Finally, as coupled atmosphere–ocean regional climate models in the Mediterranean Sea cannot be used to study the thermohaline circulation and the dense water formation driven by extreme bora events in the northern Adriatic Sea—which required a proper reproduction of the orographically-driven atmospheric dynamics—the Adriatic Sea can be used to experiment and develop new types of climate studies which may become the new state-of-the-art of coastal climate simulations.

Acknowledgements Special thanks to Roman Brogli from the Eidgenössische Technische Hochschule (ETH Zürich, Switzerland) and Laurent Li from the Université Pierre et Marie Curie (Paris, France) who provided insights concerning the pseudo-global warming (PGW) method and the regional climate model ocean-atmosphere results (from LMDZ4-NEMOMED8), respectively, used in this study. Support of the European Centre for Middle-range Weather Forecast (ECMWF) staff is greatly appreciated, in particular Xavier Abellan and Carsten Maass, as well as for ECMWF's computing and archive facilities used in this research. Finally, the authors would like to thank the two anonymous reviewers for their valuable comments. This work has been supported by projects ADIOS and BivACME (the respective Croatian Science Foundation Grants IP-2016-06-1955 and IP-2019-04-8542), CHANGE WE CARE (Interreg Italy-Croatia Programme project) and ECMWF Special Project (The Adriatic decadal and inter-annual oscillations: modelling component).

Author contributions IV and CD contributed to the study conception and design. Material preparation was done by IT and CD. Set-up of the models and simulations were performed by CD. Analysis of the results and production of the figures were performed by IT, IV and CD. The first draft of the manuscript was written by CD and all authors commented on previous versions of the manuscript. All authors read and approved the final manuscript.

Funding ADIOS project: Croatian Science Foundation Grant IP-2016-06-1955. BivACME project: Croatian Science Foundation Grant IP-2019-04-8542. CHANGE WE CARE project: Interreg Italy-Croatia Programme Grant. European Centre for Middle-range Weather Forecast (ECMWF) Special Project: The Adriatic decadal and inter-annual oscillations: modelling component.

Data availability The model results and the measurements used to produce this article can be obtained under the Open Science Framework (OSF) FAIR data repository <https://osf.io/7d6jq/> (<https://doi.org/10.17605/OSF.IO/7D6JQ>).

Compliance with ethical standards

Conflict of interest The authors declare that they have no conflict of interest.

Code availability Codes used to produce this article can be obtained under the Open Science Framework (OSF) FAIR data repository <https://osf.io/7d6jq/> (<https://doi.org/10.17605/OSF.IO/7D6JQ>).

Appendix

Physical quantities used for the description of the bora dynamics:

θ : Potential temperature (K).

r : Mixing ratio (kg/kg).

$g = 9.81$: Gravitational acceleration (m/s²).

α : Specific volume (m³/kg).

Ω : Angular velocity vector of the earth's rotation (rad/s).

\mathbf{u} : Three-dimensional wind velocity vector (m/s).

U : Horizontal wind speed (m/s).

$\theta_{va} = \theta(1 + 0.61r)$: Virtual potential temperature (K).

$N = \left(\frac{g}{\theta_{va}} \frac{\partial \theta_{va}}{\partial z} \right)^{\frac{1}{2}}$: Brunt-Väisälä frequency (1/s or Hz).

$PV = \alpha(2\Omega + \nabla \times \mathbf{u}) \cdot \nabla \theta$: Potential vorticity (PVU = 10⁻⁶ m²K/s/kg).

$F_r = \frac{U}{hN}$: Froude number, with h the height of the mountain.

Physical quantities used for the calculation of the surface heat fluxes:

U_a : Horizontal wind speed at 2 m (m/s).

T_a : Air temperature at 2 m (°C).

T_s : Sea surface temperature (°C).

r_h : Relative humidity at 2 m (%).

ρ_a : Density of moist air at 2 m (kg/m³).

P_a : Mean sea level pressure (hPa).

$e_{sat}(T)$: Saturation vapor pressure (hPa).

$L(T) = 2501000 - 2370T$: Latent heat of vaporization (J/kg).

$C_H, C_E = 0.00115$: Turbulent transfer coefficients.

$C_p = 1004.67$: Specific heat capacity (J/K/kg).

$q_a \approx \frac{0.62197(0.01 T_h e_{sat}(T_a))}{p_a}$: Air saturation specific humidity at 2 m (kg/kg).

$q_s \approx \frac{0.62197(0.98 e_{sat}(T_s))}{p_a}$: Sea surface saturation specific humidity (kg/kg).

$Q_H = \rho_a C_H C_p U_a (T_a - T_s)$: Sensible heat flux (W/m²).

$Q_E = \rho_a C_E U_a L(T_s) (q_a - q_s)$: Latent heat flux (W/m²).

References

- Artegiani A, Bregant D, Paschini E, Pinardi N, Raicich F, Russo A (1997) The Adriatic Sea general circulation. Part I. Air–sea interactions and water mass structure. *J Phys Oceanogr* 27:1492–1514. [https://doi.org/10.1175/1520-0485\(1997\)027<1492:TASGCP>2.0.CO;2](https://doi.org/10.1175/1520-0485(1997)027<1492:TASGCP>2.0.CO;2)
- Balsamo G, Albergel C, Beljaars A, Boussetta S, Brun E, Cloke H, Dee D, Dutra E, Muñoz-Sabater J, Pappenberger F, de Rosnay P, Stockdale T, Vitart F (2015) ERA-Interim/Land: a global land surface reanalysis data set. *Hydrol Earth Syst Sci* 19:389–407. <https://doi.org/10.5194/hess-19-389-2015>
- Batistić M, Garić R, Molinero JC (2014) Interannual variations in Adriatic Sea zooplankton mirror shifts in circulation regimes in the Ionian Sea. *Clim Res* 61:231–240. <https://doi.org/10.3354/cr01248>
- Beg Paklar G, Isakov V, Koracin D, Kourafalou V, Orlić M (2001) A case study of bora-driven flow and density changes on the Adriatic shelf (January 1987). *Cont Shelf Res* 21:1751–1783. [https://doi.org/10.1016/S0278-4343\(01\)00029-2](https://doi.org/10.1016/S0278-4343(01)00029-2)
- Belušić Vozila A, Güttler I, Ahrens B, Obermann-Hellhund A, Telišman Prtenjak M (2019) Wind over the Adriatic region in CORDEX climate change scenarios. *J Geophys Res Atmos* 124:110–130. <https://doi.org/10.1029/2018JD028552>
- Belušić D, Klaić ZB (2004) Estimation of bora wind gusts using a limited area model. *Tellus A* 56:296–307. <https://doi.org/10.1111/j.1600-0870.2004.00068.x>
- Belušić D, Klaić ZB (2006) Mesoscale dynamics, structure and predictability of a severe Adriatic bora case. *Meteorol Z* 15:157–168
- Belušić D, Pasarić M, Orlić M (2004) Quasi-periodic bora gusts related to the structure of the troposphere. *Q J R Meteorol Soc* 130:1103–1121. <https://doi.org/10.1256/qj.03.53>
- Beuviel J, Sevault F, Herrmann M, Kontoyiannis H, Ludwig W, Rixen M, Stanev E, Béranger K, Somot S (2010) Modeling the Mediterranean Sea interannual variability during 1961–2000: focus on the Eastern Mediterranean Transient. *J Geophys Res Atmos* 115:C08017. <https://doi.org/10.1029/2009JC005950>
- Bignami F, Sciarra R, Carniel S, Santoleri R (2007) Variability of Adriatic Sea coastal turbid waters from SeaWiFS imagery. *J Geophys Res Oceans* 112:C03S10. <https://doi.org/10.1029/2006JC003518>
- Blasniig M, Riedel B, Schiemer L, Zuschin M, Stachowitsch M (2013) Short-term post-mortality scavenging and longer term recovery after anoxia in the northern Adriatic Sea. *Biogeosciences* 10:7647–7659. <https://doi.org/10.5194/bg-10-7647-2013>
- Boldrin A, Carniel S, Giani M, Marini M, Bernardi Aubry F, Campanelli A et al (2009) Effects of bora wind on physical and biogeochemical properties of stratified waters in the northern Adriatic. *J Geophys Res Oceans* 114:C08S92. <https://doi.org/10.1029/2008JC004837>
- Carniel S, Warner JC, Chiggiato J, Sclavo M (2009) Investigating the impact of surface wave breaking on modeling the trajectories of drifters in the northern Adriatic Sea during a wind-storm event. *Ocean Model* 30(2–3):225–239. <https://doi.org/10.1016/j.ocemod.2009.07.001>
- Chen J, Wang Z, Tam C-Y, Lau N-C, Dickson Lau D-S, Mok H-Y (2020) Impacts of climate change on tropical cyclones and induced storm surges in the Pearl River Delta region using pseudo-global-warming method. *Sci Rep* 10:1965. <https://doi.org/10.1038/s41598-020-58824-8>
- Civitaresse G, Gačić M, Lipizer M, Borzelli GLE (2010) On the impact of the bimodal oscillating system (BiOS) on the biogeochemistry and biology of the Adriatic and Ionian Seas (Eastern Mediterranean). *Biogeosciences* 7:3987–3997. <https://doi.org/10.5194/bg-7-3987-2010>
- Conan P, Testor P, Estournel C, D’Ortenzio F, Pujo-Pay M, Durrieu de Madron X (2018) Preface to the Special Section: dense water formations in the northwestern Mediterranean: from the physical forcings to the biogeochemical consequences. *J Geophys Res Oceans* 123:6983–6995. <https://doi.org/10.1029/2018JC014301>
- Darmaraki S, Somot S, Sevault F et al (2019) Future evolution of Marine Heatwaves in the Mediterranean Sea. *Clim Dyn* 53:1371–1392. <https://doi.org/10.1007/s00382-019-04661-z>
- Dee DP, Uppala SM, Simmons AJ, Berrisford P, Poli P, Kobayashi S, Andrae U, Balmaseda MA, Balsamo G, Bauer P, Bechtold P, Beljaars ACM, van de Berg L, Bidlot J, Bormann N, Delsol C, Dragani R, Fuentes M, Geer AJ, Haimberger L, Healy SB, Hersbach H, Hólm EV, Isaksen L, Kållberg P, Köhler M, Matricardi M, McNally AP, Monge-Sanz BM, Morcrette JJ, Park BK, Peubey C, de Rosnay P, Tavolato C, Thépaut JN, Vitart F (2011) The ERA-Interim reanalysis: configuration and performance of the data assimilation system. *Q J R Meteorol Soc* 137:553–597. <https://doi.org/10.1002/qj.828>
- Denamiel C, Šepić J, Ivanković D, Vilibić I (2019) The Adriatic Sea and coast modelling suite: evaluation of the meteotsunami forecast component. *Ocean Model* 135:71–93. <https://doi.org/10.1016/j.ocemod.2019.02.003>
- Denamiel C, Pranić P, Quentin F, Mihanović H, Vilibić I (2020) Pseudo-global warming projections of extreme wave storms in complex coastal regions: the case of the Adriatic Sea. *Clim Dyn*. <https://doi.org/10.1007/s00382-020-05397-x>
- de Ruggiero P, Zanchettin D, Bensi M et al (2018) Water masses in the Eastern Mediterranean Sea: an analysis of measured isotopic oxygen. *Pure Appl Geophys* 175:4047–4064. <https://doi.org/10.1007/s00024-018-1850-9>
- Dunić N, Vilibić I, Šepić J, Mihanović H, Sevault F, Somot S, Waldman R, Nabat P, Arsouze T, Pennel R, Jordà G, Precali R (2019) Performance of multi-decadal ocean simulations in the Adriatic Sea. *Ocean Model* 134:84–109. <https://doi.org/10.1016/j.ocemod.2019.01.006>
- Franco P, Michelato A (1992) Northern Adriatic Sea: oceanography of the basin proper and of the western coastal zone. *Marine Coastal Eutrophication*. In: Proceedings of an International Conference, Bologna, Italy, 21–24 March 1990, pp 35–62. <https://doi.org/10.1016/B978-0-444-89990-3.50013-4>
- Gačić M, Borzelli GLE, Civitaresse G, Cardin V, Yari S (2010) Can internal processes sustain reversals of the ocean upper circulation? The Ionian Sea example. *Geophys Res Lett* 37:L09608. <https://doi.org/10.1029/2010GL043216>
- Gačić M, Civitaresse G, Miserocchi S, Cardin V, Crise A, Mauri E (2002) The open-ocean convection in the Southern Adriatic: a controlling mechanism of the spring phytoplankton bloom. *Cont Shelf Res* 22:1897–1908. [https://doi.org/10.1016/S0278-4343\(02\)00050-X](https://doi.org/10.1016/S0278-4343(02)00050-X)
- Giorgi F (2006) Climate change hot-spots. *Geophys Res Lett* 33:L08707. <https://doi.org/10.1029/2006GL025734>

- Gohm A, Mayr GJ, Fix A, Giez A (2008) On the onset of bora and the formation of rotors and jumps near a mountain gap. *Q J R Meteorol Soc* 134:21–46. <https://doi.org/10.1002/qj.206>
- González-Alemán JJ, Pascale S, Gutierrez-Fernandez J, Murakami H, Gaertner MA, Vecchi GA (2019) Potential increase in hazard from Mediterranean hurricane activity with global warming. *Geophys Res Lett* 46:1754–1764. <https://doi.org/10.1029/2018GL081253>
- Grisogono B, Belušić D (2009) A review of recent advances in understanding the meso- and microscale properties of the severe Bora wind. *Tellus A* 61:1–16. <https://doi.org/10.1111/j.1600-0870.2008.00369.x>
- Grubišić V (2004) Bora-driven potential vorticity banners over the Adriatic. *Q J R Meteorol Soc* 130:2571–2603. <https://doi.org/10.1256/qj.03.71>
- Hopkins TS, Artegiani A, Bignami F, Russo A (1999) Water-mass modification in the Northern Adriatic: a preliminary assessment from the ELNA data set. In: Hopkins TS et al (eds) *The Adriatic Sea. Ecosystem Research Report* 32, pp 3–23
- Hourdin F, Musat I, Bony S, Braconnot P, Codron F, Dufresne JL, Fairhead L, Filiberti MA, Friedlingstein P, Grandpeix JY, Krinner G, LeVan P, Li ZX, Lott F (2006) The LMDZ4 general circulation model: climate performance and sensitivity to parametrized physics with emphasis on tropical convection. *Clim Dyn* 27:787–813. <https://doi.org/10.1007/s00382-006-0158-0>
- Ionescu C, Klein RJT, Hinkel J, Kavi Kumar KS, Klein R (2009) Towards a formal framework of vulnerability to climate change. *Environ Model Assess* 14:1–16. <https://doi.org/10.1007/s10666-008-9179-x>
- Ivanov VV, Shapiro GI, Huthnance JM, Aleshin DL (2004) Cascades of dense water around the world ocean. *Prog Oceanogr* 60:47–98. <https://doi.org/10.1016/j.pocean.2003.12.002>
- Janeković I, Mihanović H, Vilibić I, Tudor M (2014) Extreme cooling and dense water formation estimates in open and coastal regions of the Adriatic Sea during the winter of 2012. *J Geophys Res Oceans* 119:3200–3218. <https://doi.org/10.1002/2014JC009865>
- Jeffries MA, Lee C (2007) A mode-based climatology of the northern Adriatic Sea. *J Geophys Res* 112:C03S02. <https://doi.org/10.1029/2006JC003664>
- Jiang Q, Doyle JD (2005) Wave breaking induced surface wakes and jets observed during a bora event. *Geophys Res Lett* 32:L17807. <https://doi.org/10.1029/2005GL022398>
- Josipović L, Obermann-Hellhund A, Brisson E, Ahrens B (2018) Bora in regional climate models: impact of model resolution on simulations of gap wind and wave breaking. *Croat Meteor J* 53:31–42
- Klemp JB, Durran DR (1987) Numerical modelling of Bora winds. *Meteorol Atmos Phys* 36:215–227. <https://doi.org/10.1007/BF01045150>
- Kokkini Z, Gerin R, Poulain P-M, Mauri E, Pasarić Z, Janeković I, Pasarić M, Mihanović H, Vilibić I (2017) A multiplatform investigation of Istrian Front dynamics (north Adriatic Sea) in winter 2015. *Medit Mar Sci* 18:344–354. <https://doi.org/10.12681/mms.1895>
- Kourafalou VH (1999) Process studies on the Po River plume, North Adriatic Sea. *J Geophys Res Oceans* 104(C12):29963–29985. <https://doi.org/10.1029/1999JC900217>
- Krasakopoulou E, Souvermezoglou E, Minas HJ, Scoullou M (2005) Organic matter stoichiometry based on oxygen consumption-nutrients regeneration during a stagnation period in Jabuka Pit (middle Adriatic Sea). *Cont Shelf Res* 25(1):127–142
- Kuzmić M, Janeković I, Book JW, Martin PJ, Doyle JD (2007) Modeling the northern Adriatic double-gyres response to intense bora wind: a revisit. *J Geophys Res Oceans* 112:C03S13. <https://doi.org/10.1029/2005JC003377>
- Kuzmić M, Grisogono B, Li X, Lehner S (2015) Examining deep and shallow Adriatic bora events. *Q J R Meteorol Soc* 141:3434–3438. <https://doi.org/10.1002/qj.2578>
- Ličer M, Smerkol P, Fettich A, Ravdas M, Papapostolou A, Mantzi-afou A, Strajnar B, Cedilnik J, Jeromel M, Jerman J, Petan S, Malačič V, Sofianos S (2016) Modeling the ocean and atmosphere during an extreme bora event in northern Adriatic using one-way and two-way atmosphere–ocean coupling. *Ocean Sci* 12:71–86. <https://doi.org/10.5194/os-12-71-2016>
- Orlić M, Dadić V, Grbec B, Leder N, Marki A, Matić F, Mihanović H, Beg Paklar G, Pasarić M, Pasarić Z, Vilibić I (2007) Wintertime buoyancy forcing, changing seawater properties and two different circulation systems produced in the Adriatic. *J Geophys Res Oceans* 112:C03S07. <https://doi.org/10.1029/2005JC003271>
- Pinardi N, Allen I, Demirov E, De Mey P, Korres G, Lascaratos A, Le Traon P-Y, Maillard C, Manzella G, Tziavos C (2003) The Mediterranean ocean Forecasting System: first phase of implementation (1998–2001). *Ann Geophys* 21:3–20. <https://doi.org/10.5194/angeo-21-3-2003>
- Poulain PM, Raicich F (2001) Forcings. In: Cushman-Roisin B (ed) *Physical oceanography of the Adriatic Sea*. Kluwer Acad, Dordrecht, pp 45–65
- Powley HR, Krom MD, Van Cappellen P (2016) Circulation and oxygen cycling in the Mediterranean Sea: sensitivity to future climate change. *J Geophys Res Oceans* 121:8230–8247. <https://doi.org/10.1002/2016JC012224>
- Prtenjak MT, Belušić D (2009) Formation of reversed lee flow over the north eastern Adriatic during bora. *Geofizika* 26:145–155
- Prtenjak MT, Viher M, Jurković J (2010) Sea-land breeze development during a summer Bora event along the north-eastern Adriatic coast. *Q J R Meteorol Soc* 136:1554–1571. <https://doi.org/10.1002/qj.649>
- Pullen J, Doyle JD, Signell RP (2006) Two-way air–sea coupling: a study of the Adriatic. *Mon Weather Rev* 134:1465–1483. <https://doi.org/10.1175/MWR3137.1>
- Pullen J, Doyle JD, Haack T, Dorman C, Signell RP, Lee CM (2007) Bora event variability and the role of air–sea feedback. *J Geophys Res* 112:C03S18. <https://doi.org/10.1029/2006JC003726>
- Raicich F, Malačič V, Celio M, Giaiotti D, Cantoni C, Colucci RR, Čermelj B, Pucillo A (2013) Extreme air–sea interactions in the Gulf of Trieste (North Adriatic) during the strong Bora event in winter 2012. *J Geophys Res Oceans* 118:5238–5250. <https://doi.org/10.1002/jgrc.20398>
- Schär C, Frei C, Lüthi D, Davies HC (1996) Surrogate climate-change scenarios for regional climate models. *Geophys Res Lett* 23:669–672. <https://doi.org/10.1029/96GL00265>
- Sherwood CR, Book JW, Carniel S, Cavalieri L, Chiggiato J, Das H, Doyle JD, Harris CK, Niedoroda AW, Perkins H, Poulain P-M, Pullen J, Reed CW, Russo A, Sclavo M, Signell RP, Traykovski P, Warner JC (2004) Sediment dynamics in the Adriatic Sea investigated with coupled models. *Oceanography* 17(4):46–57. <https://doi.org/10.5670/oceanog.2004.04>
- Signell RP, Chiggiato J, Horstmann J, Doyle JD, Pullen J, Askari F (2010) High-resolution mapping of Bora winds in the northern Adriatic Sea using synthetic aperture radar. *J Geophys Res Oceans* 115:C04020. <https://doi.org/10.1029/2009JC005524>
- Somot S, Sevault F, Déqué M (2006) Transient climate change scenario simulation of the Mediterranean Sea for the twenty-first century using a high-resolution ocean circulation model. *Clim Dyn* 27:851–879. <https://doi.org/10.1007/s00382-006-0167-z>
- Soto-Navarro J, Jordá G, Amores A, Cabos W, Somot S, Sevault F, Macias D, Djurdjević V, Sannino G, Li L, Sein D (2020) Evolution of Mediterranean Sea water properties under climate change scenarios in the Med-CORDEX ensemble. *Clim Dyn* 54:2135–2165. <https://doi.org/10.1007/s00382-019-05105-4>
- Stiperski I, Ivančan-Picek B, Grubišić V, Bajić A (2012) Complex bora flow in the lee of Southern Velebit. *Q J R Meteorol Soc* 138:1490–1506. <https://doi.org/10.1002/qj.1901>

- Trapp RJ, Hoogewind KA (2016) The realization of extreme tornadic storm events under future anthropogenic climate change. *J Clim* 29:5251–5265. <https://doi.org/10.1175/JCLI-D-15-0623.1>
- Trošić T, Trošić Z (2010) Numerical simulation and observational analysis of the wrinkles of Pag's ribs. *Bound-Lay Meteorol* 134:353–366. <https://doi.org/10.1007/s10546-009-9439-6>
- van Vuuren DP, Edmonds J, Kainuma M, Riahi K, Thomson A, Hibbard K, Hurtt GC, Kram T, Krey V, Lamarque JF, Masui T, Meinshausen M, Nakicenovic N, Smith SJ, Rose SK (2011) The representative concentration pathways: an overview. *Clim Change* 109(1–2):5–31. <https://doi.org/10.1007/s10584-011-0148-z>
- Vilibić I, Book JW, Beg Paklar G, Orlić M, Dadić V, Tudor M, Martin PJ, Pasarić M, Grbec B, Matic F, Mihanović H, Morović M (2009) West Adriatic coastal water excursions into the East Adriatic. *J Mar Syst* 78:S132–S156. <https://doi.org/10.1016/j.jmarsys.2009.01.015>
- Vilibić I, Matijević S, Šepić J, Kušpilić G (2012) Changes in the Adriatic oceanographic properties induced by the Eastern Mediterranean Transient. *Biogeosciences* 9:2085–2097. <https://doi.org/10.5194/bg-9-2085-2012>
- Vilibić I, Šepić J, Proust N (2013) Weakening thermohaline circulation in the Adriatic Sea. *Clim Res* 55(3):217–225. <https://doi.org/10.3354/cr01128>
- Vilibić I, Mihanović H, Janeković I, Šepić J (2016) Modelling the formation of dense water in the northern Adriatic: sensitivity studies. *Ocean Model* 101:17–29. <https://doi.org/10.1016/j.ocemod.2016.03.001>
- Vilibić I, Mihanović H, Janeković I, Denamiel C, Poulain P-M, Orlić M, Dunić N, Dadić V, Pasarić M, Muslim S, Gerin R, Matic F, Šepić J, Mauri E, Kokkini Z, Tudor M, Kovač Ž, Džoić T (2018) Dense water formation in the coastal northeastern Adriatic Sea: the NAdEx 2015 experiment. *Ocean Sci* 14:237–258. <https://doi.org/10.5194/os-14-237-2018>
- Vosper S, Ross A, Renfrew I, Sheridan P, Elvidge A, Grubišić V (2018) Current challenges in orographic flow dynamics: turbulent exchange due to low-level gravity-wave processes. *Atmosphere* 9:361. <https://doi.org/10.3390/atmos9090361>
- Warner JC, Armstrong B, He R, Zambon JB (2010) Development of a coupled ocean-atmosphere-wave-sediment transport (COAWST) modeling system. *Ocean Model* 35:230–244. <https://doi.org/10.1016/j.ocemod.2010.07.010>
- Zängl G, Hornsteiner M (2007) Can trapped gravity waves be relevant for severe foehn windstorms? A case study. *Meteorol Z* 16:203–212. <https://doi.org/10.1127/0941-2948/2007/0199>
- Zore-Armanda M, Gačić M (1987) Effects of Bora on the circulation in the north Adriatic. *Ann Geophys* 5B:93–102

Publisher's Note Springer Nature remains neutral with regard to jurisdictional claims in published maps and institutional affiliations.